

EPSC2017
OPS3 abstracts

THE AMMONIA ABSORPTION VARIATIONS ON JUPITER IN 2005-2015

V. Tejfel, V. Vdovichenko, G. Kirienko, A. Karimov, P. Lysenko, V. Filippov, G. Kharitonova, A. Khozhenetz
 Fessenkov Astrophysical Institute, Almaty, Kazakhstan (tejf@mail.ru)

Abstract

We measured the intensity of the 645 and 787 nm NH_3 absorption bands in five latitudinal belts of Jupiter (STZ, SEB, EZ, NEB and NTZ) during almost full period of its revolution around the Sun: from 2005 to 2015. The variations in the equivalent widths of the bands were investigated. The permanently lowered intensity of the 787 nm NH_3 band in NEB is confirmed. There are also some systematic differences in latitudinal and temporal variations between the 645 and 787 nm ammonia bands.

1. Introduction

In 2014 we first detected on Jupiter a strange depression in absorption in the 787 nm NH_3 absorption band in the Northern hemisphere at low latitudes [1,2]. The similar feature was noted with radio observations at the millimeter wave range [3, 4] as enhanced brightness temperature in the NEB. That may be considered as an evidence of decreased ammonia abundance at the lower northern latitudes on Jupiter. Based on our spectral observations of Jupiter from 2005 to 2015, we carried out a preliminary analysis of the data about spatial-temporal variations of the 645 and 787 nm NH_3 absorption bands over this period. These data were derived from the measurements in five main belts of Jupiter: the Southern and Northern Tropical Zones (STZ and NTZ), the Southern and Northern Equatorial Belts (SEB and NEB) and the Equatorial Zone (EZ).

2. The spectral observations and their processing

The CCD-spectrograms of the central meridian of Jupiter were selected for processing the spectra of the five measured zones. In general, 600 zonal spectra with a width of 15 pixels or about 3.7 arc sec on the disk of Jupiter were measured. The measurements of the ammonia absorption bands are certainly rather difficult, since they are overlapped with more extended methane bands. The 787 nm NH_3 absorption band was extracted with using of ratios of the Jovian

spectra to the Saturn's disk spectrum that was taken as a reference. "Clear" profiles of the NH_3 bands are shown in Figure 1.

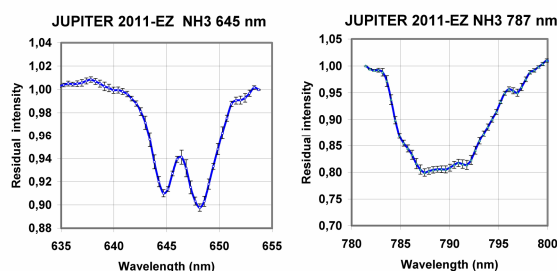


Figure 1: The examples of the NH_3 absorption bands profiles

The result of the measurements consisted in obtaining the estimates of the absorption bands' equivalent widths and variations in their values over zones and years. The average values of the equivalent widths for all measurements are: $W = 6.24 \pm 0.59 \text{ \AA}$ for the 645 nm NH_3 band; $W = 17.98 \pm 1.37 \text{ \AA}$ for the 787 nm NH_3 band. But over different years and zones the observed variations behave differently.

3. Main results and discussion

Figure 2 shows histograms of temporal (annual) changes in ammonia absorption separately in each of the five investigated belts of Jupiter. To compare the zonal behavior of absorption over the years, the data are plotted in Figure 3. One can see that the absorption variations are not the same for these two bands of ammonia. As in our other studies, the latitudinal variations for the two bands are obviously different. A lowered absorption of ammonia in the 787 nm band in the NEB remains a peculiar feature, repeated every year. Unlike the thermal radio emission, when a cloud layer does not affect its passage, the formation of the NH_3 bands in the visible spectral range depends noticeably not only on the local content of gaseous ammonia, but also on the properties of the scattering cloud bulk. Perhaps the differences in the

behaviour of these bands are related to this, although it is strange that a more intense 787 nm band shows a better agreement with the data of radio observations.

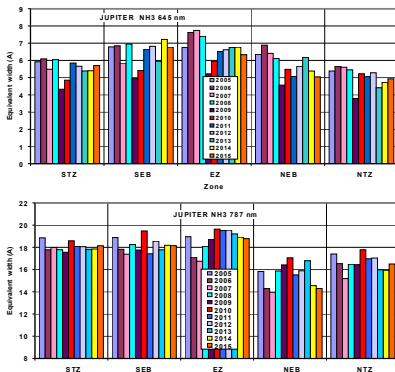


Figure 2: The annual variations of the 645 and 787 nm NH_3 bands' equivalent widths.

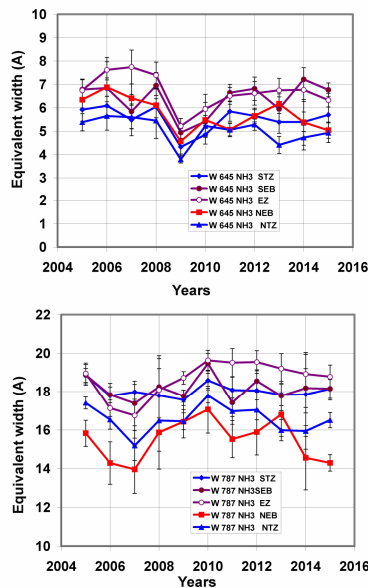


Figure 3: A comparison of temporal variations of the NH_3 absorption in the five Jovian latitudinal belts.

Figure 4 shows the relative values for both NH_3 absorption bands averaged over all years and normalized to EZ. The depression of absorption in the 787 nm band in the NEB manifests itself quite clearly, and on the average it reaches about 20 percent.

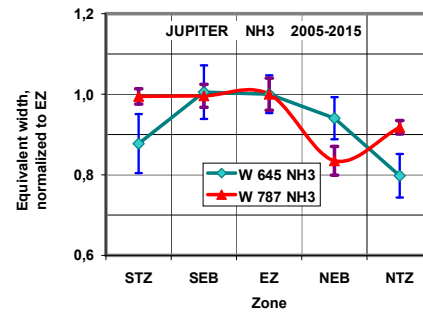


Figure 4: The ammonia absorption bands' intensities averaged over time and normalized to EZ.

From the measurements of these bands and from the data on the brightness temperatures in the infrared [4] and radio [5] ranges of thermal radiation, one can see the longitudinal variations exist. Their study, especially from the standpoint of significant changing the content of gaseous ammonia at different latitudes and longitudes, is very important and interesting. So, all the results obtained stimulate the continuation of further more detailed studies.

Acknowledgements

This work was prepared according the grant 0073/GF4 Ministry of Science and Education of Kazakhstan Republic.

References

- [1] Tejfel V. , Karimov A.M., Vdovichenko V.D. Strange latitudinal variations of the ammonia absorption on Jupiter . Bull.AAS,Vol. 37, p.682., 2005
- [2] Tejfel V..et al. Spatially resolved variation in the methane and ammonia absorption in the atmosphere of Jupiter . As-tron.and Astrophys.Transactions ,Vol. 24, pp.359-363., 2005
- [3] Showman A., de Pater, I. Dynamical implications of Jupiter's tropospheric ammonia abundance. Icarus, Vol. 174, pp. 192-204, 2005
- [4] de Pater I. et al. Peering through Jupiter's clouds with radio spectral imaging. Science,Vol. 352, lpp.1290-1294, 2016
- [5] Fletcher L. et al.. Mid-infrared mapping of Jupiter's temperatures, aerosol opacity and chemical distributions with IRTF/TEXES . Icarus,Vol. 278, pp.128-161, 2016

Latest Results on Jupiter's Atmosphere and Radiation Belts from the Juno Microwave Radiometer

Michael A. Janssen (1), Scott J. Bolton (2), Steve M. Levin (1), Virgil Adumitroaie (1), Michael D. Allison (3), John K. Arballo (1), Sushil K. Atreya (4), Amadeo Bellotti (5), Shannon T. Brown (1), Samuel Gulkis (1), Andrew P. Ingersoll (6), Laura A. Jewell (1), Cheng Li (1), Liming Li (7), Jonathan Lunine (8), Sidharth Misra (1), Glenn S. Orton (1), Fabiano A. Oyafuso (1), Daniel Santos-Costa (2), Edwin Sarkissian (1), Paul G. Steffes (5), Ross Williamson (1), and Zhimeng Zhang (1)
 (1) Jet Propulsion Laboratory, California Institute of Technology, Pasadena CA 91108
 (2) Southwest Research Institute, San Antonio TX 78228
 (3) Goddard Institute of Space Studies, New York NY 10025
 (4) University of Michigan, Ann Arbor MI 48109
 (5) Georgia Institute of Technology, Atlanta GA 30332
 (6) California Institute of Technology, Pasadena CA 91125
 (7) University of Houston, Houston TX 77004
 (8) Cornell University, Ithaca NY 14853

Abstract

The Juno Microwave Radiometer (MWR) was designed to investigate Jupiter's atmosphere and radiation belts as one of a suite of instruments that form the core of the Juno mission [1]. Results from the first seven periapsis passes on the atmosphere and the radiation belts will be summarized.

1. Introduction

Jupiter's neutral atmosphere is shrouded by clouds that are impervious to all but microwave radiation. Our view from Earth is impeded further by intense synchrotron radiation that obscures all but the shortest-wavelength microwave radiation emanating from above the few-bar pressure level of the atmosphere. Juno's highly elliptical polar orbit allows the MWR to avoid these obstacles by observing the atmosphere during a periapsis pass from a vantage point between Jupiter and the radiation belts. This enables the measurement of longer-wavelength atmospheric thermal radiation from pressure depths of hundreds of bars, and also provides a unique view of the inner radiation belts that enables a more complete study of their structure.

2. Observational Approach

The MWR comprises six radiometric channels operating at wavelengths from 1.4 cm to 50-cm wavelength. The MWR antennas are mounted on the sides of the spinning Juno spacecraft so that they observe along the sub-spacecraft track as the

spacecraft moves from north to south through periapsis. Collectively they sample the thermal emission from pole to pole with better than 1° resolution in latitude at periapsis, and from the cloud tops to pressures as deep as a few hundred bars. Figure 1 shows the contribution functions for atmospheric thermal emission measured by the six MWR channels assuming a nominal model for the atmosphere.

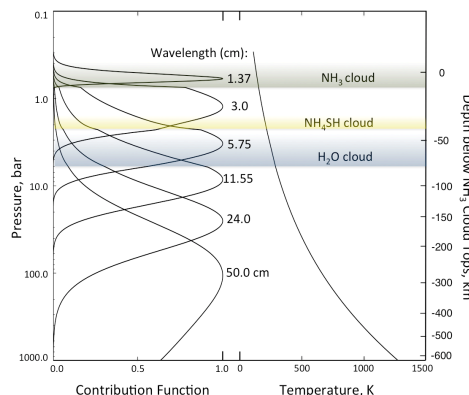


Figure 1: Contribution functions for the six MWR channels for a nominal atmospheric model.

The observational data are the mean radiances in the antenna beams converted by Planck's law to blackbody temperatures and accordingly given in units of Kelvin (antenna temperatures). For atmospheric data these are corrected for the beam averaging to obtain source brightness temperatures,

or the effective mean radiance of Jupiter in the beam at the boresight axis, for each observation. The absolute accuracy of each measurement is 2%, uncorrelated among channels, while the relative accuracy at each wavelength is 0.1%. The radiation belt data consist of antenna temperatures from latitudinal scans from a (mostly) radiation-free perspective inside the belts.

3. Data Products

The atmospheric scans along the spacecraft subtrack yield both absolute brightness temperatures and, since many points are observed over a range of emission angles, their dependence on emission angle. The data products derived from these data include latitudinal tracks of absolute nadir brightness temperatures, where off-nadir measurements are extrapolated to nadir using their simultaneously-obtained emission angle dependencies; and emission angle dependence in terms of limb-darkening parameters. The former are useful in the determination of large-scale structure in the subcloud atmosphere due to opacity variations, which are not limited by 2% absolute uncertainties. These also are useful in the constructions of partial 3D maps, which show brightness structure as a function of latitude, longitude, and wavelength (a proxy for depth). Emission-angle dependencies allow fine structure with depth to be obtained with accuracy limited only by the 0.1% relative accuracies of the measurements at each wavelength. The radiation belt data consist of antenna temperatures from latitudinal scans from a radiation-free perspective inside the belts, useful for comparison with synthetic data obtained by computations using parameterized models of the belts.

4. Results

The trace of absolute nadir brightness temperature for the first perijove pass has been used to infer a striking variation in the distribution of NH_3 , which is the dominant source of microwave opacity in the atmosphere [2]. This variation implies a previously unexpected deep circulation with exciting implications for gas giant planets in general.

The accumulation of data from subsequent perijove passes will be shown to demonstrate the longitudinal, temporal, and depth dependencies of observed structures. Partial 3D maps will show the structure and depths of specific features on Jupiter, notably the polar regions and the Great Red Spot. Finally, efforts underway to exploit the limb-darkening measurements in search of water will be described.

Acknowledgements

The work described in this paper was conducted at the Jet Propulsion Laboratory (JPL), California Institute of Technology, under contract with the National Aeronautics and Space Administration (NASA). The author wishes to thank the numerous contributors from the Juno Project and the Lockheed-Martin spacecraft team, without whom this ambitious project would not have been possible.

References

- [1] Janssen, M.A., et al., MWR: Microwave Radiometer for the Juno Mission to Jupiter, Space Science Reviews, 2017 doi: 10.1007/s11214-017-0349-5
- [2] Bolton, S.J. et al., Jupiter's interior and deep atmosphere: the first close polar pass with the Juno spacecraft, Science, in press, 2017.

Overview of Juno Results at Jupiter

S. Bolton (1), J. Connerney (2,3), S. Levin (3) and the Juno Science Team

(1) SWRI, San Antonio, United States, (2) Space Research Corporation, Annapolis, MD, USA, (3) NASA Goddard Space Flight Center, Greenbelt, MD, USA, (4) JPL, Caltech, Pasadena, United States (sболton@swri.edu)

Abstract

Juno is the first mission to investigate Jupiter using a close polar orbit. The Juno science goals include the study of Jupiter interior composition and structure, deep atmosphere and its polar magnetosphere. All orbits have perijove at approximately 5000 km above Jupiter's visible cloud tops. The payload consists of a set of microwave antennas for deep sounding, magnetometers, gravity radio science, low and high-energy charged particle detectors, plasma wave antennas, ultraviolet imaging spectrograph, infrared imager and spectrometer and a visible camera.

1. Introduction

The primary science goal of Juno is the understanding of the origin and evolution of Jupiter, the history of our solar system and the more general theory of planetary system formation. To address these goals, Juno probes significantly below the cloud decks to constrain its interior structure using measurements of Jupiter's gravity and magnetic fields and deep atmospheric composition [1]. Juno's elliptical orbit provides multiple periapsis passes very close to Jupiter, on a pole-to-pole trajectory. The very close-in polar orbits enable a unique exploration of Jupiter's polar magnetosphere [2]. Juno's payload of science investigations include an X-band and Ka-band communications subsystem for determining Jupiter's gravity field, dual magnetometers to map Jupiter's internal magnetic field, a set of microwave radiometers to probe Jupiter's deep atmosphere, a visible color camera and an infrared spectrometer/imager and ultraviolet spectrograph/imager to capture views of Jupiter. Juno also carries a suite of fields and particle instruments for in-situ sampling Jupiter's magnetosphere and investigating its powerful aurora [2].

2. Science Results

On July 4, 2016, the Juno spacecraft arrived at Jupiter to begin the investigation of Jupiter. The spacecraft acquired science observations of Jupiter, passing within 3000 km of the equatorial cloud tops. Images of Jupiter's poles indicate cyclonic activity unique to the solar system. Microwave sounding reveals weather features, dominated by an ammonia-rich, narrow low-latitude plume. Near-infrared mapping reveals the relative humidity within prominent down-welling regions. Juno's measured gravity field differs significantly from the current knowledge and is one order of magnitude more precise. This has implications for the distribution of heavy elements in the interior including the existence and mass of Jupiter's core. The observed magnetic field exhibits smaller spatial variations than expected. Direct observations of the Jovian polar magnetosphere provide the first close-up observations of Jupiter's auroral regions. Energetic particle and plasma detectors measured electrons precipitating in the polar regions, exciting intense aurorae, observed simultaneously by the ultraviolet and infrared imaging spectrographs.

Acknowledgements

The authors acknowledge financial support from the Juno project under NASA, CNES and ASI.

References

- [1] Bolton, S. J., Adriani, A., Adumitroaie, V., et al.: Jupiter's interior and deep atmosphere: the first pole-to-pole pass with the Juno spacecraft, *Science*, in press, 2017.
- [2] Connerney, J., Adriani, A., Allegrini, F., et al.: Jupiter's Magnetosphere and Aurorae Observed by the Juno Spacecraft During its First Polar Orbits, *Science*, in press, 2017.

Transient brightening of Jupiter's aurora observed by the Hisaki satellite and Hubble Space Telescope during approach phase of the Juno spacecraft

T. Kimura^{1*}, J. D. Nichols², R. L. Gray³, C. Tao⁴, G. Murakami⁵, A. Yamazaki⁵, S. V. Badman³, F. Tsuchiya⁶, K. Yoshioka⁷, H. Kita⁶, D. Grodent⁸, G. Clark⁹, I. Yoshikawa¹⁰, and M. Fujimoto^{5,11}
¹Nishina Center for Accelerator-Based Science, RIKEN, Hirosawa, Saitama, Japan, ²Department of Physics and Astronomy, University of Leicester, Leicester, UK, ³Department of Physics, Lancaster University, Lancaster, UK, ⁴National Institute of Information and Communications Technology, Tokyo, Japan, ⁵Institute of Space and Astronautical Science, Japan Aerospace Exploration Agency, Sagami, Japan, ⁶Planetary Plasma and Atmospheric Research Center, Tohoku University, Sendai, Japan, ⁷Department of Earth and Planetary Science, Graduate School of Science, University of Tokyo, Tokyo, Japan, ⁸Université de Liège, Liège, Belgium, ⁹The Johns Hopkins University Applied Physics Laboratory, Laurel, Maryland, USA, ¹⁰Department of Complexity Science and Engineering, University of Tokyo, Kashiwa, Japan, ¹¹Earth-Life science Institute, Tokyo Institute of Technology, Tokyo, Japan *Correspondence to: tomoki.kimura@riken.jp

Abstract

[1] In early 2014, continuous monitoring with the Hisaki satellite discovered transient auroral emission at Jupiter during a period when the solar wind was relatively quiet for a few days. Simultaneous imaging made by the Hubble Space Telescope (HST) suggested that the transient aurora is associated with a global magnetospheric disturbance that spans from the inner to outer magnetosphere. However, the temporal and spatial evolutions of the magnetospheric disturbance were not resolved because of the lack of continuous monitoring of the transient aurora simultaneously with the imaging. Here we report the coordinated observation of the aurora and plasma torus made by Hisaki and HST during the approach phase of the Juno spacecraft in mid-2016. On day 142, Hisaki detected a transient aurora with a maximum total H₂ emission power of ~8.5 TW. The simultaneous HST imaging was indicative of a large 'dawn storm', which is associated with tail reconnection, at the onset of the transient aurora. The outer emission, which is associated with hot plasma injection in the inner magnetosphere, followed the dawn storm within less than two Jupiter rotations. The monitoring of the torus with Hisaki indicated that the hot plasma population increased in the torus during the transient aurora. These results imply that the magnetospheric disturbance is initiated via the tail reconnection and rapidly expands toward the inner magnetosphere, followed by the hot plasma injection reaching the plasma torus. This corresponds to the radially inward transport of the plasma and/or energy from the outer to the inner magnetosphere.

Acknowledgements

This study performed on the basis of the NASA/ESA Hubble Space Telescope (proposal ID: GO14105), obtained at the Space Telescope Science Institute, which is operated by AURA, Inc. for NASA. The data of Hisaki satellite is archived in the Data Archives and Transmission System (DARTS) JAXA. TK was supported by a Grant-in-Aid for Scientific Research (16K17812) from the Japan Society for the Promotion of Science. JDN was supported by STFC Fellowship (ST/I004084/1) and STFC grant ST/K001000/1. RLG was supported by an STFC Studentship. CT was supported by a Grant-in-Aid for scientific research from the Japan Society for the Promotion of Science (JSPS, 15K17769). SVB was supported by STFC Fellowship ST/M005534/1. HK was supported by a Grant-in-Aid for Scientific Research (26287118 and 15H05209) from the Japan Society for the Promotion of Science.

References

- [1] **Tomoki Kimura**, J. D. Nichols, R. L. Gray, C. Tao, G. Murakami, A. Yamazaki, S. V. Badman, F. Tsuchiya, K. Yoshioka, H. Kita, D. Grodent, G. Clark, I. Yoshikawa, and M. Fujimoto (2017 under review), Transient brightening of Jupiter's aurora observed by the Hisaki satellite and Hubble Space Telescope during approach phase of the Juno spacecraft, *Geophysical Research Letters*, 2017GL072912.

Jupiter cloud morphology and zonal winds from ground-based observations during Juno's first year around Jupiter

R. Hueso [ricardo.hueso@ehu.es] (1), A. Sánchez-Lavega (1), J. M. Gómez-Forrellad (2), J. F. Rojas (1), S. Pérez-Hoyos (1), J. F. Sanz-Requena (3), J. Peralta (4), I. Ordonez-Etxeberria (1), H. Chen-Chen (1), I. Mendikoa (1), D. Peach (5), C. Go (6), A. Wesley (7), P. Miles (8) and T. Olivetti (9)

(1) Dpto. Física Aplicada I, Escuela de Ingeniería de Bilbao, UPV/EHU, Bilbao, Spain, (2) Fundació Observatori Esteve Duran, Seva, Barcelona, Spain, (3) Dpto. de Ciencias Experimentales, Universidad Europea Miguel de Cervantes, Valladolid, Spain, (4) Institute of Space and Astronautical Science (ISAS/JAXA), Japan. (5) British Astronomical Association, Burlington House, London, UK, (6) Physics Department, University of San Carlos, Cebu City, Philippines, (7) Astronomical Society of Australia, School of Physics, University of Sydney, Sydney, Australia, (8) Gemeye Observatory, Rubyvale, Australia, (9) Unioni Astrofili Italiani, Rome, Italy.

Abstract

Jupiter's upper atmosphere displays a variety of meteorological phenomena at a wide range of spatial scales. Changes, local and global, occur at several time-scales and affect differently the cloud and hazes observable at different vertical altitudes sampled in the visible and in weak and strong methane absorption bands. Ground-based observations are required to understand the meteorological activity in the long time spans between high-resolution observations attained by Juno and other powerful observational means like the Hubble Space Telescope (HST). We here report the evolution of meteorological systems in the planet over 2017. We base our analysis on the following sources: (i) Observations obtained by our PlanetCam UPV/EHU instrument on the 2.2-m telescope at Calar Alto Observatory in Spain and covering the spectral range from 0.38 to 1.7 μm ; (ii) Observations attained with small telescopes by amateur astronomers including images acquired with 1-m size telescopes and covering the 0.4 to 1.0 μm range. We focus our analysis on the following topics: (a) Dynamics of the South Equatorial Belt outbreak since December 2016; (b) Changed colors of the North Temperate Belt following a planetary-scale disturbance that largely finished by November 2016; (c) Global winds and their evolution from December 2015 to April 2017; (d) Short-scale waves at the North Equatorial Belt; (e) Dynamics of the polar regions above 60 deg latitudes.

1. Introduction

Prior to and during Juno's first perijove ground-based and HST/OPAL observations show that Jupiter was

in a quiescent normal state [1]. The only exception was a longitudinally limited small northwards latitudinal expansion of the North Equatorial Belt (NEB) that has been linked to thermal waves in the upper atmosphere [2]. This situation broke in October 2016 with the nearly simultaneous outburst of four moist convective plumes in the North Temperate Belt (NTB) that grew to a planetary scale disturbance that evolved until November 2016 [3] changing the colors and morphology of the NTB. Instead of resuming to a quiescent state a large outburst of activity in the South Equatorial Belt started at the end of December 2016 and progressed at least until late April 2017. Short-scale wave features, similar to gravity waves previously found in HST observations in 2015 [4], were observed by several amateur astronomers since February 2017 and at least up to April 2017 in the North Equatorial Belt (NEB).

2. Planetcam images

PlanetCam UPV/EHU is a dual camera that uses the lucky imaging technique at the 2.2-m telescope in Calar Alto observatory in Southern Spain. The light from the telescope is separated by a dichroic mirror and is sent into two detectors in the wavelength ranges 0.38-1.0 μm (visible) and 1.0-1.7 μm (Short wave infrared, SWIR) [5-6]. Fast images (10-50 images per second) improve the spatial resolution over the seeing by a factor of 4 and long exposures are used in narrow band filters sampling several weak intermediate and strong methane absorption bands. We ran one Jupiter observing campaign in 26-31 March 2016 and a similar campaign is scheduled for June 2016; another one has being requested in July 2016. Images were calibrated with observations

of spectrophotometric standard stars and enable the study of the vertical distribution of clouds and hazes and the spatial distribution of colors.

3. Amateur observations

Amateur observers constitute a major source of high-quality observations of Jupiter. High-quality amateur images were downloaded from the PVOL2 database (<http://www.pvol2.ehu.es>) [7] and ALPO Japan (<http://alpo-j.asahikawa-med.ac.jp/indexE.htm>).

These images were used to measure zonal winds in different moments in time over 2016-2017 exploring small-scale changes in the winds associated to the activity at the SEB outbreak and the aftermath of the NTB planetary-scale disturbance.

5. Results

We present zonal winds from -75 to $+74$ degrees planetographic latitudes from ground-based Planetcam and amateur images obtained over several months in 2017. We compare these zonal winds with previous wind retrievals over similar data from December 2015 to May 2016 [1]. We explore changes in the zonal winds associated to the past activity in the NTB [3] and to the current disturbance in the SEB.

We present color indices from PlanetCam photometrically calibrated images as a tool to quantify the different colors in the NTB to the rest of the planet and its usual state [8].

We discuss the NEB waves observed from February to April 2017. Amateur observations showed several systems of wavy features with typical wavelengths of $1-2^\circ$ in the North Equatorial Belt close to the location of convective outbreaks. This was the first time such waves were observed by amateurs, but similar systems have been observed in the past in HST images [3] and in data from several spacecrafts. We present the visual characteristics of these features and their characterization as gravity waves from a comparison with theoretical expectations for gravity waves in Jupiter.

We also present polar maps of the planet in a variety of filters. In particular, PlanetCam observations in the SWIR channel are very effective to show structures at high latitudes. We compare polar maps of the planet at a variety of deeply penetrating image filters showing vortices up to ± 73 deg latitudes and methane

absorption bands showing polar waves in the upper hazes [9]. These global maps of the polar regions, together with the rest of the analysis presented, can provide a global context to JunoCam observations of the planet [10].

Acknowledgements

This work has been supported by the Spanish project AYA2015-65041-P (MINECO/FEDER, UE), Grupos Gobierno Vasco IT-765-13 and UFI11/55 from UPV/EHU. JP thanks JAXA's International Top Young Fellowship.

References

- [1] Hueso et al.: Jupiter cloud morphology and zonal winds from ground-based observations before and during Juno's first perijove, *Geophys. Res. Lett.*, 44, doi:10.1002/2017GL073444 (in press).
- [2] Fletcher et al.: Jupiter's North Equatorial Belt expansion and thermal wave activity ahead of Juno's arrival, *Geophys. Res. Lett.*, 44, doi:10.1002/2017GL073421 (in press).
- [3] Sánchez-Lavega et al.: A planetary-scale disturbance in the most intense Jovian atmospheric jet from JunoCam and ground-based observations, *Geophys. Res. Lett.* (in press).
- [4] Simon et al.: First results from the Hubble OPAL Program: Jupiter in 2015, *ApJL*, 812(1), id55, 8 (2015).
- [5] Sánchez-Lavega et al.: PlanetCam UPV/EHU: A simultaneous visible and near infrared lucky-imaging camera to study solar system objects, *Proc. of SPIE*, 8446, 84467X-1-84467-X-9 (2012).
- [6] Mendikoa, I.: PlanetCam UPV/EHU: A Two-channel Lucky Imaging Camera for Solar System Studies in the Spectral Range $0.38-1.74 \mu\text{m}$, *PASP*, 128 (961), 0350002 (2016).
- [7] Hueso et al.: The Planetary Virtual Observatory and Laboratory (PVOL) and its integration into the Virtual European Solar and Planetary Access (VESPA), *PSS* (in press).
- [8] Ordóñez-Etxeberria et al.: Spatial distribution of Jovian clouds, hazes and colors from Cassini ISS multi-spectral images, *Icarus*, 267, 34-50 (2016).
- [9] Sánchez-Lavega et al.: A system of circumpolar waves in Jupiter's stratosphere, *Geophys. Res. Lett.*, 25, 4043-4046 (1998).
- [10] Orton et al.: The first close-up images of Jupiter's polar regions: Results from the Juno mission JunoCam instrument, *Geophys. Res. Lett.*, 44, doi:10.1002/2016GL072443 (in press).

Results of Joint Observations of Jupiter's Atmosphere by Juno and a Network of Earth-Based Observing Stations

G. Orton (1), T. Momary (1), F. Tabataba-Vakili (1), S. Bolton (2), S. Levin (1), A. Adriani (3), G. R. Gladstone (2), C. Hansen (4), M. Janssen (1), and the Juno-Supporting Observing Team
 (1) Jet Propulsion Laboratory, California Institute of Technology, Pasadena, California, USA, (2) Southwest Research Institute, San Antonio, Texas, USA, (3) Instituto de Astrofisica e Planetologia, Spaziali, Rome, Italy, (4) Planetary Science Institute, Tucson, Arizona, USA

Abstract

Well over sixty investigator/instrument investigations are actively engaged in the support of the Juno mission. These observations range from X-ray to the radio wavelengths and involve both space- and ground-based astronomical facilities. These observations enhance and expand Juno measurements by (1) providing a context that expands the area covered by often narrow spatial coverage of Juno's instruments, (2) providing a temporal context that shows how phenomena evolve over Juno's 53-day orbit period, (3) providing observations in spectral ranges not covered by Juno's instruments, and (4) monitoring the behavior of external influences to Jupiter's magnetosphere. Intercommunications between the Juno scientists and the support program is maintained by reference to a Google table that describes the observation and its current status, as well as by occasional group emails. A non-interactive version of this invitation-only site is mirrored in a public site. Several sets of these supporting observations are described at this meeting.

1. Motivation

The Juno mission coordinates a network of Earth-based observations including Earth-proximal, Earth-orbiting, airborne and ground-based facilities, to extend and enhance the scientific return of the mission. The spectral range of this program covers X-ray through radio wavelengths, and it currently involves over 60 investigator / facility pairs. The observations (1) cover spectral regions not included in Juno's instrumentation, (2) provide spatial context for Juno's often spatially limited coverage of Jupiter, and (3) describe the evolution of atmospheric features measured only once or separated by long time intervals by Juno, and (4) measure the extent of external influences on the magnetosphere.

2. Organization

The program is coordinated at JPL. Coordination of the investigations is done sometimes by group email, but the status of programs is given by modifications to a Google Table listing contemplated, proposed, planned and completed observations. The table is hosted by Radical Media, Inc., in association with the general Mission Juno website, and it is curated by Glenn, Tom and Fachreddin. The table is continuously updatable and updated by the individual contributing investigators or contact-representatives of their teams. Investigators interested in participating in this program email one of us and are subsequently invited to the Google site to contribute and indicate the status of their programs. These plans are publicly available on a continuously (every 5 minutes) updated, non-interactive mirror of this site: <https://www.missionjuno.swri.edu/planned-observations>. An example of a graphical table of contemporaneously acquired data is shown in Figure 1. The investigations are listed by mission phase, beginning with approach and segmented by orbit, with one extra time in January 2017, when a suite of observations remained that were scheduled to support a previously planned orbit in the original 14-day orbit plan.

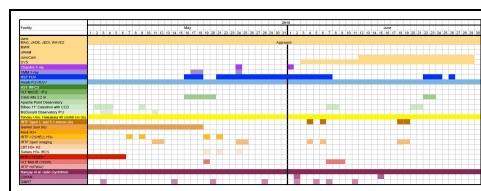


Figure 1: Example of planning table from the approach phase.

3. Highlights

Here we describe examples of results showing instances of useful Earth-based supporting observations benefiting the mission or new discoveries made by the observations themselves.

3.1 Approach

The Juno approach to Jupiter in 2016 provided the rare opportunity to observe auroral activity at Jupiter simultaneously with in-situ measurements of upstream solar-wind characteristics. Simultaneous auroral characteristics from the HST STIS instrument and interplanetary data from Juno were made. On DoY 142, HST observed the most powerful auroras ever observed by the telescope. Three solar-wind compression regions were observed. The first, on DoY 142, is near an enhancement in Jupiter's sodium nebula on DoY 140 and with an eruption observed on Io on DoY 138. The power emitted by the noon active region did not show any dependence on any interplanetary parameter. Details are given by Nichols et al. [1]. Combined observations of X-ray emission were also taken between 17 May and 1 June, showing a regular pulsing south-polar counterpart to a north-polar emission region [2].

Perijove 2

Although Jupiter was less than 17° from the sun, the NASA Infrared Telescope Facility (IRTF) obtained images, including those at $2.16\ \mu\text{m}$ and $3.8\ \mu\text{m}$, that verified the development of a very unusual disturbance in Jupiter's North Temperate Belt (NTB) that was suggested by lower-resolution images from JunoCam's approach movie. Details are given by [3].

Frequent IRTF observations at these and other diagnostic wavelengths continue in an ongoing program and are hosted by the Juno Science Operations Center at <http://junoirtf.space.swri.edu>.

Perijove 4

Observations from the NIRI instrument on Gemini N that were stabilized against atmospheric seeing by adaptive optics (AO) extended upward in altitude a sensitivity to particulate properties from the JunoCam "methane" filter at $0.89\ \mu\text{m}$ (Figure 2, left panel). Although not nearly the same spatial resolution as the JunoCam imaging, they showed

clearly the vertical changes in morphology of the stratospheric haze generated by auroral-related chemistry that is partly entrained by a polar vortex. In fact, in some of the strongest gaseous absorption at $2.17\ \mu\text{m}$ they showed an optically thick inner "core" of the haze with particles implied to be higher than the rest - a new discovery (Figure 2, right panel).

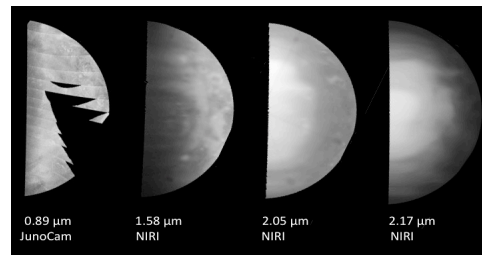


Figure 2: Polar projection of JunoCam "methane" filter image on PJ4 (2017 Feb 2), together with AO-stabilized images of Jupiter on 2017 Jan 30, taken at the Gemini North Telescope using NIRI.

4. Summary and Conclusions

The support program continues to be successful in the four areas outlined. Several more examples will be illustrated, including updates through the current perijove of Juno at the meeting.

Acknowledgements

This research was funded by the National Aeronautics and Space Administration through the Juno Project. A portion of these funds were distributed to the Jet Propulsion Laboratory, California Institute of Technology.

References

- [1] Nichols, J. et al. Response of Jupiter's auroras to conditions in the interplanetary medium as measured by the Hubble Space Telescope and Juno. *Geophys. Research Lett.* In press. doi 10.1002/2017GL073029.
- [2] Dunn, W. et al. Discovery of Jupiter's southern auroral x-ray hot spot – An uncorrelated counterpart to the north. *Nature Geosci.* 2017. In press.
- [3] Sanchez-Lavega, A. et al. A planetary-scale disturbance in the most intense Jovian atmospheric jet from JunoCam and ground-based observations. *Geophys. Research Lett.* In press. 2017. doi 10.1002/2017GL073421.

Properties and circulation of Jupiter's circumpolar cyclones as measured by JunoCam

G. S. Orton (1), G. Eichstädt (2), J. H. Rogers (3), C. J. Hansen (4), M. Caplinger (5), T. Momary (1), F. Tabataba-Vakili (1), A. P. Ingersoll (6)

(1) Jet Propulsion Laboratory, California Institute of Technology, Pasadena, California USA (glenn.orton@jpl.nasa.gov), (2) Independent scholar, Stuttgart, Germany, (3) British Astronomical Association, London, UK, (4) Planetary Science Institute, Tucson, Arizona, USA, (5) Malin Space Science Systems, San Diego, California, USA, (6) California Institute of Technology, Pasadena, California, USA.

Abstract

JunoCam has taken the first high-resolution visible images of Jupiter's poles, which show that each pole has a cluster of circumpolar cyclones (CPCs), each one separated in longitude by roughly equal spacing [1]. There are five at the south pole and eight at the north pole. These configurations, including their asymmetries and the characteristics of individual cyclones, have remained stable over 7 months from perijove 1 to perijove 5 as of this writing. Each cyclone has a circular outline with a prominent system of trailing spiral arms. In the north, the internal morphology of adjacent cyclones alternates from one to the next. Angular motions within each cyclone appear to be similar to each other but quite different from vortices at lower latitudes.

1. Introduction

Although nominally intended as a vehicle for Juno-mission outreach, the JunoCam instrument is Juno's visible-light camera, providing the first high-resolution (50-70 km/pixel) imaging of Jupiter's poles. These revealed a visibly darker background than banded structure at lower latitudes, with mostly brighter features that were dominated by cyclonic features that included chaotic "folded filamentary features" (FFRs) and more compact ovals. One of the surprises in these images was the appearance of clusters of circular spirals within 6° of both of Jupiter's poles, a morphology not seen elsewhere on the planet. These were labelled as circumpolar cyclones (CPCs). We report here a more detailed study of their properties over the orbits since their characterization in the first perijove (PJ1) by Orton et al. [1]. JunoCam observations are limited to the daylight portion of the polar hemisphere and so are complementary to JIRAM observations of 5- μ m thermal emission from polar regions covering all longitudes but limited to fewer perijoves.

2. Data

JunoCam is rigidly mounted on the spinning spacecraft. That way, it can take a full panorama within about 30 seconds consisting of up to 82 narrow exposures. Usually, it takes partial panoramas of the target of interest. The camera has a horizontal field of view of about 58°, and Kodak KAI-2020 CCD sensor with four filter stripes, a red, a green, a blue and a narrow-band 890-nm infrared filter attached on the 1600x1200 light-sensitive pixels. For each of the four filters, there is an according readout region of 1600x128 pixels which can be transferred into the resulting raw image. This transfer isn't immediate, but the 12-bit data number of each pixel is encoded as an 8-bit value, and tiles of 16x16 pixels are compressed either lossy or lossless. Usually, the encoding of the 12-bit data as an 8-bit value is nonlinear according to a companding function. Motion blur is mostly avoided by a technique called time delay integration (TDI). In RGB mode, for each exposure, three of the four readout regions are added as stripes to the raw image. Further details about the instrument and its operation are available in Hansen et al. [2]

Observations were made in both north and south polar regions in perijoves PJ1, PJ3, PJ4, PJ5, and we anticipate more subsequent to this writing. Polar imaging in PJ5 was and PJ6 is scheduled over extended periods of time in order to cover more longitudes as the planet rotates through daylight, and to enable time-lapse measurements that include measurements of rotation of the CPCs.

3. Methods

With an approximate geometrical camera model, including its pointing for each exposure, the appropriate 3D vector was calculated for each pixel in a given reference frame, e.g. J2000. Position and pointing information are inferred from SPICE data, with some manual adjustment. Jupiter is modeled as a

MacLaurin spheroid on Jupiter's 1-bar level. A planetocentric coordinate system assigns a 3D position to each longitude/latitude pair. The 3D vector, pointing from Juno to the 3D position, completes the connection of each longitude / latitude pair to color information. With this method, each raw JunoCam image of Jupiter is reduced to an approximately geometrically calibrated polar map projection.

Because Jupiter is rotating and Juno is moving rapidly, the illumination for each JunoCam image changes rapidly. Comparison of images requires approximate normalization of the images. For now, this is achieved in a heuristic way, essentially stretching contrast over regions of approximately similar solar incidence angles, subtracting the mean brightness for these bins, and accounting for changing light scattering of a presumed haze layer as a function of emission angle, which can be obtained for sufficiently small crops by high-pass filtering. Further nonlinear brightness stretch and saturation enhancement brings out detail, and helps distinguish bluish haze from reddish cloud tops. Additional registering and stacking enhanced the signal-to-noise ratio. Similar processing of consecutive images allows for animations revealing motion, as well as for quantitative analysis of cloud velocities. Figure 1 shows an example from PJ4.

4. Results

We confirm the results of the initial JunoCam report [1] that the CPCs are clustered around each pole with approximately equal spacing in longitude. At the south pole, a cluster of five CPCs has an additional cyclone at the center, but it is slightly offset from the position of the pole. The center of the north polar cluster of eight CPCs is not seen, as it is in darkness at this time. The configuration of the CPCs in both poles appears to be stable over the perijoves (PJs) observed as of this writing (PJ1, PJ3, PJ4, PJ5), spanning 27 August 2016 through 27 March 2017. The cyclones are all roughly circular with prominent trailing spiral arms whose cyclonic appearance is verified by time-lapse imaging. They very much resemble terrestrial hurricanes but are larger, with diameters of ~5800-8000 km. The northern cyclones have alternating properties from one to the next, as suggested by PJ1 observations. Angular rotation rates and wind speeds within the cyclones have been measured over intervals of 15-72 minutes as a function of radius; they appear quantitatively similar to each other, but remarkably different from vortices at lower latitudes.

As of this writing, we continue to work on the quantitative details and interpretation of these intriguing and unexpected features that will be discussed in detail in our presentation.

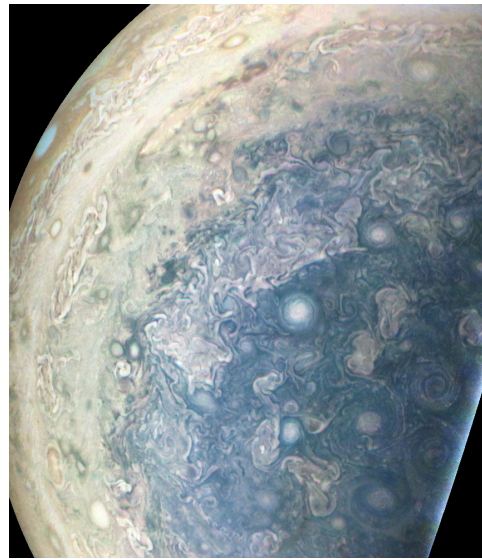


Figure 1. Map-projected color image of Jupiter centered over the south pole from PJ4 with first-order corrections for solar illumination angle variations and processing to enhance details. CPCs surround the pole in the lower right.

Acknowledgements

This research was funded by the National Aeronautics and Space Administration through the Juno Project. A portion of these funds were distributed to the Jet Propulsion Laboratory, California Institute of Technology.

References

- [1] Orton, G. S., Hansen, C., Caplinger, M., Ravine, M., Atreya, S., Ingersoll, A. P., Jensen, E., Momary, T., Lipkman, L., Krysak, D., Zimdar, R., Bolton, S. The first close-up images of Jupiter's polar regions: results from the Juno mission JunoCam instrument. *Geophys. Res. Lett.* 44, 2017. doi: 10.1002/2016GL072443.
- [2] Hansen, C. J., M. A. Caplinger, A. Ingersoll M. A. Ravine, E. Jensen, S. Bolton, G. Orton. Junocam: Juno's outreach camera. *Space Sci. Rev.* 2014. doi:10.007/s/11214-014-0079-x

Absorption of Ammonia (NH₃) in the visible/near-infrared reflectance spectrum of Jupiter

P.G.J. Irwin (1), R. Garland (1) and A. Braude (1)

(1) Atmospheric, Oceanic and Planetary Physics, University of Oxford, Parks Road, Oxford OX1 3PU, UK

Abstract

Observations of the visible/near-infrared reflectance spectrum of Jupiter have been made with VLT/MUSE in the spectral range 0.48 – 0.93 μm , in support of the NASA/Juno mission. These spectra contain spectral signatures of gaseous ammonia (NH₃), whose abundance above the cloud tops can thus be determined if we have reliable information on the its absorption spectrum. While there are a number of sources of NH₃ absorption data in this spectral range, they cover small sub-ranges, which do not necessarily overlap and have been determined from a variety of sources. There is thus considerable uncertainty regarding the consistency of these different sources when modelling the reflectance of the entire visible/near-IR range. In this paper we will analyse the VLT/MUSE observations of Jupiter to determine the optimal way of modelling the absorption of ammonia.

1. Introduction

The reflectance spectrum of Jupiter contains a number of absorption features of ammonia gas at 550 nm, 650nm, and then further bands increasing in strength from 740 nm to 1000 nm. In support of the NASA/Juno mission we have recently observed Jupiter with the MUSE instrument at the Very Large Telescope, which records complete visible/near-IR spectra (0.48 – 0.93 μm) from all points on the observable disc. Given reliable information on the strength of these bands we can use these wavelengths to determine the abundance of ammonia above the cloud tops. However, available data come from a range of sources whose consistency with respect to each other has not been properly tested. In this paper we assess the consistency of these data sets.

1.1 VLT/MUSE Observations

The MUSE instrument at the Very Large Telescope in Chile is an Integral Field Spectrograph, which records images of 300×300 resolution from a field of view of $60'' \times 60''$ (in wide field mode), but where each pixel contains a complete visible/near-IR spectrum (0.48 – 0.93 μm) with a spectral resolving power of ~ 3000 . The observations of Jupiter recorded by MUSE have excellent spatial resolution (due to the location of VLT) as can be seen in Fig.1.

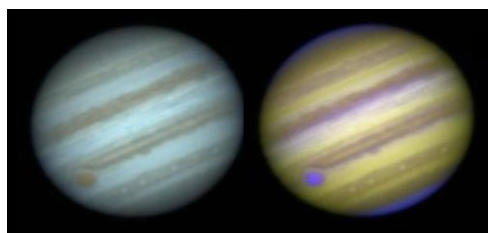


Figure 1: Left: Colour-composite MUSE image constructed from data recorded in March 2016. The GRS is clearly visible at lower left. Right: False-colour image, where red is reflection at 630 nm (weak methane absorption), green is reflection at 510 nm (sensitive to blue-absorbing 'chromophores'), and blue is reflection at 890nm (strong methane absorption, sensitive only to high level hazes).

Figure 2 shows a typical spectrum extracted from the MUSE data for a zone together with the spectrum modeled with our NEMESIS[3] radiative transfer and retrieval tool, using ammonia data [1] and [4]. To show the location of the ammonia features, Fig. 2. also shows the spectrum calculated with the ammonia abundance increased.

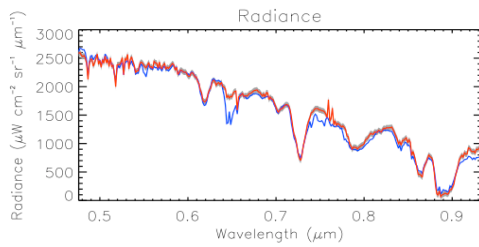


Figure 2. Typical MUSE spectrum (and estimated error) shown in grey, with the fit of our NEMESIS retrieval model shown in red. The blue line is the modelled spectrum calculated with an increased abundance of ammonia, showing the position of the ammonia features.

2. Data Sources

There are four main sources of ammonia absorption data in this spectral region. The data reported by Bowles et al. (2008)[1], Giver et al. (1975)[2] and Lutz and Owen (1980)[4] come from measuring the absorption of ammonia gas in a laboratory path at medium or high resolution and fitting either band models [1], mean absorptions [2,4] or in one case line strengths[2] for a selection of the strongest lines. In most cases (except [1]) these observations are limited to be near room temperature and thus it is difficult to know how well they may be extended to the colder temperatures on Jupiter. In addition they are measured under self-broadening conditions only, rather than H_2/He -broadening as experienced in Jupiter's atmosphere. The 550 nm band is only reported by [4], while the 640 nm band is reported by both [4] and [2]. The laboratory data of Bowles et al. (2008)[1] covers wavelengths longer than 740 nm in the form of band model coefficients, which have some temperature dependence. More recently the ExoMOL project has computed an *ab initio* line table for NH_3 from first principals [5]. These data cover wavelengths longer than 800 nm, but include line strengths and lower state energies only. Hence, further analysis and assumptions have to be made in order to assign line widths (under H_2/He -broadening conditions) and also the temperature dependence of these line widths.

3. Conclusion

In this paper we will assess the reliability and consistency of these different sources of ammonia absorption data when modelling the reflectance spectra of Jupiter from our VLT/MUSE observations. We will analyse the likely temperature dependence of the data and also assess the possible corrections needed to account for broadening by an H_2/He atmosphere under Jovian conditions. Finally, we will make recommendations on the optimal combination of these data sources when analyzing the visible/near-infrared spectra of cool Jupiter-like planets in our own solar system and, as exoplanetary observations improve, of such planets about other stars also.

Acknowledgements

We would like to acknowledge the support of the UK's Science and Technology Facilities Council.

References

- [1] Bowles, N., Calcutt, S., Irwin, P., and Temple, J.: Band parameters for self-broadened ammonia gas in the range 0.74 to 5.24 μm to support measurements of the atmosphere of the planet Jupiter, *Icarus* 196, 612 – 624, 2008.
- [2] Giver, L.P., Miller, J.H., and Boese, R.W.: A laboratory atlas of the $5\nu_1$ NH_3 absorption band at 6475Å with applications to Jupiter and Saturn, *Icarus* 25, 34 – 48, 1975.
- [3] Irwin, P.G.J., et al.: The NEMESIS planetary atmosphere radiative transfer and retrieval tool. *J.Q.S.R.T.* 109, 1136 – 1150, 2008.
- [4] Lutz, B.L., and Owen, T.: The visible bands of Ammonia: Band strengths, curves of growth, and the spatial distribution of Ammonia on Jupiter. *Astrophys. J.* 235, 285 – 293, 1980.
- [5] Yurchenko, S.N., Barber, R.J., Tennyson, J.: A variationally computed line list for hot NH_3 , *Mon. Not. R. Astron. Soc.* 413, 1828–1834, 2011.

CDPP support to the Juno and Cassini missions: data access and valorization by models and tools

N. André (1), V. Génot (1), E. Budnik (2), M. Bouchemit (1), M. Gangloff (1), M. Blanc (1), P. Louarn (1)

(1) IRAP, CNRS-UPS, 9 avenue du colonel Roche, 31028 Toulouse, France; (2) Noveltis, Ramonville Saint Agne, France (nicolas.andre@irap.omp.eu / Fax: +33-5-61-55-83-70)

Abstract

Thanks to their unique orbital geometry, the Juno and the Cassini proximal orbits will allow for the first time a quantitative study of the characteristics of the magnetosphere-ionosphere coupling at Jupiter and Saturn.

We will report the status of our current technical and scientific efforts in order to integrate in the CDPP system (<http://www.cdpp.eu>) the Juno and Cassini datasets recently released by the NASA/Planetary Data System (<https://pds-ppi.igpp.ucla.edu/>) in order to enhance the science return of these missions. The CDPP proposes a set of tools and models aiming at valorizing the variety of its datasets.

The CDPP/AMDA (Automated Multi-Dataset Analysis, <http://amda.cdpp.eu>) tool is a web-based facility for on line analysis of space physics data (heliosphere, magnetospheres, planetary environments).

The CDPP/3DView (<http://3dview.cdpp.eu>) is a science tool that offers immediate 3D visualization of spacecraft position and attitude, planetary ephemerides, as well as scientific data representation (observations and models).

The CDPP/Propagation tool (<http://propagationtool.cdpp.eu>) enables to track solar storms, streams and energetic particles in the heliosphere, and predict their arrival time at planets and probes.

These tools are publicly available to the scientific community.

Juno Waves observations at Jupiter

W. S. Kurth (1), G. B. Hospodarsky (1), M. Imai (1), S. S. Tetrick (1), D. A. Gurnett (1), S.-Y. Ye (1), P. Louarn (2), P. Valek (3,4), F. Allegrini (3,4), J. E. P. Connerney (5), B. H. Mauk (6), S. J. Bolton (3), S. M. Levin (7), A. Adriani (8), G. R. Gladstone (3,4), D. J. McComas (3,9), and P. Zarka (10)
(1) University of Iowa, Iowa City, IA, USA, (2) IRAP, Toulouse, France, (3) Southwest Research Institute, San Antonio, TX, USA, (4) Department of Physics and Astronomy, University of Texas at San Antonio, San Antonio, TX, USA, (5) NASA Goddard Space Flight Center, Greenbelt, MD, USA, (6) The Johns Hopkins University Applied Physics Laboratory, Laurel, MD, USA, (7) Jet Propulsion Laboratory, Pasadena, CA, USA, (8) INAF-Istituto di Astrofisica e Planetologia Spaziali, Roma, Italy, (9) Princeton University, Princeton, NJ, USA, (10) LESIA, Observatoire de Paris, Meudon, France (william-kurth@uiowa.edu / Fax: 319-335-1753)

Abstract

The Juno spacecraft successfully entered Jupiter orbit on 5 July 2016. One of Juno's primary objectives is to explore Jupiter's polar magnetosphere. An obvious major aspect of this exploration includes remote and in situ observations of Jupiter's auroras and the processes responsible for them. To this end, Juno carries a suite of particle, field, and remote sensing instruments. One of these instruments is a radio and plasma wave instrument called Waves, designed to detect one electric field component of waves in the frequency range of 50 Hz to 41 MHz and one magnetic field component of waves in the range of 50 Hz to 20 kHz. Juno has now made scientific observations on several perijove passes beginning with Perijove 1 on 27 August 2016. This paper presents some of the early observations of the Juno Waves instrument.

Among radio emissions, kilometric, hectometric, and decametric emissions have been observed. From a vantage point at high latitudes, many of Jupiter's auroral radio emissions appear as V-shaped emissions in frequency-time space with vertices near the electron cyclotron frequency where the emissions intensify. We present observations suggesting Juno has flown through or close to several sources of these auroral radio emissions [1]. While the sources are typically found on field lines threading the main auroral oval, during Perijove 5 the geometry is consistent with a source near the Io flux tube, or the Io flux tube wake. Measurements by the Jovian Auroral Distributions Experiment (JADE) provide evidence of loss-cone electron distributions at some sources that are sufficient to drive the cyclotron maser instability [2]. Remote observations provide

source locations for broadband kilometric radiation that are consistent with auroral field lines [3].

Waves observes whistler-mode hiss on auroral field lines and over the polar cap [4]. The hiss sometimes exhibits quasi-periodic intensity fluctuations in the range of a few to a few tens of minutes, similar to that of quasi-periodic (QP) radio bursts and temporal variations in some UV auroral emissions and X-ray hot spots poleward of the main oval. The hiss intensity exhibits a good correlation with upgoing energetic electrons observed by the Jupiter Energetic particle Detector (JEDI) [5]. It is enticing to consider the possibility that the hiss and energetic electrons are associated with the quasi-periodic emissions.

Juno's perijove passes carry it over high mid-latitudes where lightning is known to exist and, subsequently, lightning whistlers have been observed. Because of the strong magnetic field and the short propagation path through relatively low density plasma, the whistler dispersion is small; typical durations of the whistlers are of order 10 ms. Proton whistlers have also been observed on a few occasions, a first for this phenomenon in a non-terrestrial locale.

We also discuss observations of dust encountered in and near the equator. Collisions with dust grains with a spacecraft speed near 60 km/s results in the vaporization of the grain and even a small part of the target material creating a hot, instantly ionized gas. The result is an impulse easily detected by the Waves instrument. It is thought that these are micron-sized and are the result of material moving inward from Jupiter's ring.

Finally, we note more distant observations of the Jovian magnetosphere and its interaction with the solar wind as revealed by upstream plasma waves, encounters with the bow shock, and many magnetopause crossings highlighted by the appearance or disappearance of continuum radiation trapped in the low-density cavity in Jupiter's distant magnetosphere [6].

References

[1] Kurth, W.S., et al.: A new view of Jupiter's auroral radio spectrum, *Geophys. Res. Lett.*, in press, doi: 10.1002/2017GL072889, 2017.

[2] Louarn, P., et al.: Generation of the jovian hectometric radiation: First lessons from Juno, *Geophys. Res. Lett.*, in press, doi: 10.1002/2017GL072923, 2017.

[3] Imai, M., et al.: Direction finding measurements of Jovian broadband and narrowband kilometric radiation from the Juno Waves instrument near Perijove 1, *Geophys. Res. Lett.*, submitted, 2017.

[4] Tetrick, S.S.: Plasma waves in Jupiter's high latitude regions: Observations from the Juno spacecraft, *Geophys. Res. Lett.*, in press, doi: 10.1002/2017GL073073, 2017.

[5] Mauk, B.H., et al.: Juno observations of energetic charged particles over Jupiter's polar regions: Analysis of mono- and bi-directional electron beams, *Geophys. Res. Lett.*, in press, doi: 10.1002/2016GL072286, 2017.

[6] Hospodarsky, G.B., et al.: Jovian bow shock and magnetopause encounters by the Juno spacecraft, *Geophys. Res. Lett.*, in press, doi: 10.1002/2017GL073177, 2017.

Preliminary Results from the JIRAM Observations of Jupiter Poles acquired during the first orbit of Juno

B.M. Dinelli¹, F. Fabiano^{1,7}, A. Adriani², A. Mura², M.L. Moriconi^{1,2}, F. Altieri², G. Sindoni², G. Filacchione², F. Tosi², A. Migliorini², G. Piccioni², R. Noschese², A. Cicchetti², S.J. Bolton³, J.E.P. Connerney⁴, S.K. Atreya⁵, D. Turrini², S. Stefani², C. Plainaki⁶, A. Olivieri⁶ and M. Amoroso⁶.

1. CNR-Istituto di Scienze dell'Atmosfera e del Clima, Bologna e Roma, Italy
2. INAF-Istituto di Astrofisica e Planetologia Spaziali, Roma, Italy
3. Southwest Research Institute, San Antonio, Texas, USA
4. NASA Goddard Space Flight Center, Greenbelt, Maryland, USA
5. University of Michigan, Ann Arbor, Michigan, USA
6. Agenzia Spaziale Italiana, Roma, Italy
7. Dipartimento di Fisica e Astronomia, Università di Bologna, Bologna, Italy

Abstract

Throughout the first orbit of the NASA Juno mission around Jupiter, the Jupiter InfraRed Auroral Mapper (JIRAM - Adriani et al. 2014) observed the northern and southern polar regions several times. The observations have been carried out in nadir and slant viewing by the L filtered imager and the spectrometer, both part of the JIRAM instrument, producing a very high number of images and spectra. The observations of the Jovian North and South Pole auroras have enabled the identification of the emissions of H_3^+ (trihydrogen cation) and CH_4 (methane). The geographical coverage of the main ovals has been partial, but sufficient to determine different regions of temperature and abundance of the H_3^+ ion from its emission lines in the wavelength range of 3-4 μm . The observations of the southern aurora have been collected in daytime only, while the northern observations cover the full Jupiter day of about 10 hours. The direct comparison of the North/South auroras shows that the Southern hemisphere auroral emissions were always more powerful than the northern ones. In the southern hemisphere the average integrated radiance was $(0.89 \pm 0.46) \times 10^{-4} \text{ W/m}^2/\text{sr}$ with the highest values reaching $7.34 \times 10^{-4} \text{ W/m}^2/\text{sr}$ while in the North no values greater than $3.38 \times 10^{-4} \text{ W/m}^2/\text{sr}$ have been found with a mean value of $(0.75 \pm 0.34) \times 10^{-4} \text{ W/m}^2/\text{sr}$. The analysis method, described by Dinelli et al. (2017), has enabled to obtain both column density (CD) and Temperature for the H_3^+ emission. The analysis of the high spatial resolution of JIRAM measurements has enabled to show that the aurora is asymmetric on both poles, with CD and temperature ovals not superimposed and not exactly located where models and previous observations suggested. On the North, the main oval averaged CDs of H_3^+ span between $1.8 \times 10^{12} \text{ cm}^{-2}$ and $2.8 \times 10^{12} \text{ cm}^{-2}$, while the retrieved temperatures show values between 800 and 950 K. On the South, the averaged CDs assume values from $2.0 \times 10^{12} \text{ cm}^{-2}$ and $3.5 \times 10^{12} \text{ cm}^{-2}$, and Temperatures from 850 and 1100 K. JIRAM indicates a complex relationship among H_3^+ CDs and Temperatures. The analysis method developed for the retrieval of H_3^+ temperature and abundances has also enabled to estimate the effective temperature of the methane peak emission (500 K in the North and 650 K in the South) and the distribution of its spectral contribution in the polar regions. The enhanced methane emission is located inside the auroral ovals in both the two hemispheres. The larger CH_4 temperature in the South would imply either higher emission altitudes or a warmer atmospheric structure than in the North. The location of the northern and southern methane enhancements appear located well inside the auroral ovals and in a narrow range of longitudes, although the limited coverage of the South Pole prevents a definite conclusion. If this pattern will

be confirmed from the next observations, it would suggest that the excitation leading to the infrared emission is linked to magnetospheric phenomena and in particular to the auroral particle precipitation in the polar caps.

The presence of C_2H_2 and C_2H_6 , reported by Altieri et al. (2016), has been investigated with negative results. It is likely that the coverage of JIRAM of Jupiter's poles during the first Juno orbit has been insufficient to detect the emissions of these hydrocarbons or that the spectral region where C_2H_2 and C_2H_6 emit was contaminated by the scattered sunlight that may have masked the faint emissions of those molecules.

Acknowledgments

The project JIRAM is funded by the Italian Space Agency.

References

Adriani et al. (2014), JIRAM, the Jovian Infrared Auroral Mapper. *Space Sci. Rev.*, doi:10.1007/s11214-014-0094-y.

Altieri et al. (2016), Mapping of hydrocarbons and H_3^+ emissions at Jupiter's north pole using Galileo/NIMS data, *Geophys. Res. Lett.*, doi:10.1002/2016GL070787.

Dinelli, B.M., et al. (2017), Preliminary Results from the JIRAM Auroral Observations taken during the first Juno orbit: 1 - Methodology and Analysis Applied to the Jovian Northern Polar Region, *Geophys. Res. Lett.*, doi:10.1002/2017GL072929.

Non-auroral altitude profiles of H_3^+ density and temperature at Jupiter

L. Moore (1), J. O'Donoghue (2), H. Melin (3), and T. Stallard (3)

(1) Boston University, Center for Space Physics, Massachusetts, USA (moore@bu.edu) ; (2) Goddard Space Flight Center, Greenbelt, USA; (3) Department of Physics and Astronomy, University of Leicester, Leicester, UK

Abstract

Over the past few decades the H_3^+ ion has proven to be a tremendously valuable probe of giant planet upper atmospheres. Auroral H_3^+ emissions at Jupiter, Saturn, and Uranus have been regularly monitored by ground-based IR telescopes, and low-latitude H_3^+ emissions have also recently revealed intriguing ionospheric coupling processes from above (particle flow from Saturn's rings) and below (an upper-atmospheric hotspot above Jupiter's Great Red Spot).

High spectral resolution observations can be used to derive the density and temperature of the emitting H_3^+ . The main remote diagnostic of planetary ionospheres, the technique of radio occultations, yields altitude profiles of electron density, yet only near the terminator of the giant planets. Therefore, direct measurements of the density of a major giant planet ion – potentially at anywhere on the sunlit hemisphere – is a valuable complementary constraint. Moreover, it is difficult to measure upper-atmospheric temperature remotely, and as H_3^+ is thought to be predominantly in local thermodynamic equilibrium with the neutral atmosphere, it can also provide insight into global giant planet energetics.

Despite the valuable scientific contributions from both space-based and ground-based observations of H_3^+ , there is a fundamental ionospheric diagnostic missing: the variation with altitude. Aside from a few limited limb-viewing geometries, all historical H_3^+ observations sample only the column-integrated ionospheric H_3^+ density and temperature.

We present two new derivations of non-auroral H_3^+ altitude profiles at Jupiter based on recent Keck observations. These derivations are focused on 55N and 20S degrees planetocentric latitude. First, the spectral slit overhangs the planet's limb, and altitude

structure is determined by inverting the density/temperature values derived by fitting a model spectrum to the data. This method requires an assumption of spherical symmetry, and application of a standard “onion-peeling” technique. Second, we combine a 1-D model of Jupiter's ionosphere with the H_3^+ observations in order to derive altitude profiles of density and temperature. This approach uses the model in order to fix the shape of the H_3^+ density profile, an assumption that is justified by the relatively simplistic nature of the photoionization and subsequent chemistry of the H_3^+ ion and validated by comparison to the altitude profile from the first approach. (Note, however, that it is currently only valid at non-auroral latitudes, as ionization due to particle precipitation introduces too many unknowns.)

As H_3^+ is predominantly in local thermodynamic equilibrium with the neutral atmosphere, this method can in principle be used to derive an estimate of the neutral temperature profile wherever H_3^+ can be detected. This further increases the value of H_3^+ observations as a probe of giant planet upper atmospheres, especially from the ground, as there will be a dearth of spacecraft at the giant planets between the end of the Cassini and Juno missions and the arrival of the JUICE and Europa Clipper missions.

Model-guided quantitative analysis of Juno's observations of MeV-energy electrons at Jupiter

D. Santos-Costa (1), H. Becker (2), P. Kollmann (3), C. Paranicas (3), B. Mauk (3), S. J. Bolton (1), S. M. Levin (2), J. L. Joergensen (4), A. Adriani (5), S. Gulkis (2), M. A. Janssen (2), R. M. Thorne (6), and J. E. P. Connerney (7,8)

(1) Southwest Research Institute, Space Science Department, United States, (2) Jet Propulsion Laboratory, California Institute of Technology, Pasadena, CA, United States, (3) The Johns Hopkins University Applied Physics Laboratory, Laurel, MD, United States, (4) DTU Space, National Space Institute, Technical University of Denmark, Kgs Lyngby, Denmark, (5) INAF, Istituto di Astrofisica e Planetologia Spaziali, Rome, Italy, (6) Retired, (7) Space Research Corporation, Annapolis, MD, United States, (8) NASA Goddard Space Flight Center, Greenbelt, MD, United States (dsantoscosta@swri.edu)

Abstract

We describe how assimilation of radiation belt data, from high energy radiation environment measurements inferred from instruments' background noise (i.e. the Radiation Monitoring data sets: SRU, ASC, and JIRAM) and Juno JEDI particle instrument (SSD and SSDs witness-shielded detectors), with radiation belt models are used to improve our knowledge about how MeV-energy electrons are distributed near the inner edge of trapping regions at Jupiter. Our preliminary cross-examination of inferred data sets indicates which data sets can be implemented in our work as model constraints for the magnetospheric region beyond Io's orbit, and those available to validate our model predictions close to the planet. In this paper, data sets from Juno's first two science passes (i.e. PJ1 and PJ3) and models of electrons belts are combined to describe the MeV-energy electron populations at high latitudes and near loss cones inside $\sim 15 R_J$. We discuss how a better understanding of Jupiter's MeV-energy electron distributions in energy, pitch-angle, and L-shell helps to improve models of Jupiter's synchrotron emission which in turn supports Juno MWR investigation of Jupiter's microwave emissions.

Acknowledgements

This work was sponsored by Southwest Research Institute, the Jet Propulsion Laboratory/California Institute of Technology, and the Johns Hopkins University Applied Physics Laboratory under contracts with the National Aeronautics and Space Administration.

Jupiter's polarized synchrotron radiation: from Earth's and Juno's measurements to theoretical modeling

D. Santos-Costa (1), S. Gulkis (2), A. Ingersoll (3), M. A. Janssen (2), S. J. Bolton (1), S. M. Levin (2), V. Adumitroaie (2), F. Oyafuso (2), S. Brown (2), R. Williamson (2), and J. E. P. Connerney (4,5)

(1) Southwest Research Institute, Space Science Department, United States, (2) Jet Propulsion Laboratory, California Institute of Technology, Pasadena, CA, United States, (3) California Institute of Technology, Pasadena, CA, United States, (4) Space Research Corporation, Annapolis, MD, United States, (5) NASA Goddard Space Flight Center, Greenbelt, MD, United States (dsantoscosta@swri.edu)

Abstract

Since late August 2016, measurements of Jupiter's microwave radiation have been taken at high data rates with the Microwave Radiometer (MWR) instrument during Juno's passes at the planet. In addition to providing unprecedented measurements of the planet's thermal emission at $\sim 1\text{-}50$ cm wavelengths, Jupiter's electron-belt synchrotron emission has also been measured with high resolution for $+90$ to -90 degrees latitude within $2 R_J$ from the planet and from inside/outside the electron-belt region. We report results and analyses of MWR data sets for the first science passes to interpret the measurements of the synchrotron radiation's linear components from a wide range of points of view. Our ability to simulate the polarized components of Jupiter's synchrotron radiation is first evaluated with Very Large Array observations of Jupiter at different radio bands. We present our data processing and reconstructions of polarized maps of Jupiter's synchrotron radiation. The simulated polarized maps are compared to Earth-based observations.

Acknowledgements

This work was sponsored by Southwest Research Institute, the Jet Propulsion Laboratory/California Institute of Technology, and the California Institute of Technology under contracts with the National Aeronautics and Space Administration.

Juno/JIRAM infrared observations of Jupiter Aurorae: results of the first year.

A. Mura¹, A. Adriani¹, F. Altieri¹, B.M. Dinelli², M.L. Moriconi², A. Migliorini¹, S.J. Bolton³, J.E.P. Connerney⁴, J-C. Gerard⁵, A. Cicchetti¹, R. Noschese¹, G. Sindoni¹, F. Tosi¹, G. Filacchione¹, F. Fabiano², G. Piccioni¹, D. Turrini¹, M. Amoroso⁶, C. Plainaki⁶, and A. Olivieri⁶

1. INAF-Istituto di Astrofisica e Planetologia Spaziali, Roma, Italy
2. CNR-Istituto di Scienze dell'Atmosfera e del Clima, Bologna / Roma, Italy
3. Southwest Research Institute, San Antonio, Texas, USA
4. NASA Goddard Space Flight Center, Greenbelt, Maryland, USA
5. Université de Liège, Belgium.
6. Agenzia Spaziale Italiana, Roma, Italy

Abstract

JIRAM (Jovian Infrared Auroral Mapper) is an imaging spectrometer on board the Juno spacecraft, which started the prime mission around Jupiter on August 2016. JIRAM is composed of two IR imager channels (L band and M band) and one spectrometer in the range 2-5 μm , with a spectral resolution of less than 10 nm. The surface resolution of both the spectrometer (1D resolution) and the imager (2D) is, when Juno is close to Jupiter's poles, as low as 50 km. Combined with the unique vantage point provided by Juno, JIRAM observed the aurora with an unprecedented resolution. In fact, the Jovian aurorae are the primary scientific goal of JIRAM. Such aurorae are the most powerful among the planets in the Solar System, resulting from high-energy electrons falling along the planet's magnetic field lines into the upper atmosphere, leading to the formation of excited H_3^+ , which then emit at different wavelengths. In particular, the main auroral oval emission is believed to be associated with upward field-aligned currents, driven by the breakdown of corotation between the planet and the plasma sheet. Such plasma is partially supplied as neutral gas by Io's volcanic activity.

JIRAM spectral range is designed to observe the auroral emission due to the H_3^+ ion. H_3^+ main roto-vibrational band has several possible transitions in the range 3.0-5.0 μm ; however, observation of the infrared emission of H_3^+ is mainly possible in a spectral interval (3.2 to 4.0 μm) where the solar and thermal radiance emitted by the planet are very low due to the intense atmospheric methane absorption band, resulting in a high auroral contrast against Jupiter's dark disk.

For this reason, one of the two imager channels (L band) is centered at 3.455 μm (in the H_3^+ emission region). Images (256 x 432 pixels) are acquired every 30 seconds (one Juno rotation) to give a context information of auroral emission, for better understanding the spectrometer data, which allows, among others, retrieval of the H_3^+ column density and temperature.

Here we show results on JIRAM's data after one year of observations. Taking advantage of different orbital configurations of the Juno spacecraft during the year, these observations provide spatial, spectral and temporal distribution of the Jovian auroras. In addition to the study of the main oval, the footprints of Io, Europa and Ganymede have also been observed and characterized.

The 2016 outbreak on Jupiter's North Temperate Belt and jet from ground-based and Juno imaging

J.H. Rogers (1), G.S. Orton (2), G. Eichstädt (3), M. Vedovato (4), M. Caplinger (5), T.W. Momary (2), C. J. Hansen (6)

(1) British Astronomical Association, London, UK; (2) Jet Propulsion Laboratory, California Institute of Technology, Pasadena, California USA; (3) Independent scholar, Stuttgart, Germany; (4) JUPOS team; (5) Malin Space Science Systems, San Diego, California, USA; (6) Planetary Science Institute, Tucson, Arizona, USA. [jrogers11@btinternet.com]

Abstract

A new outbreak of convective plumes on the peak of Jupiter's fastest jet, which had been predicted the previous year, began in autumn, 2016. It was observed just after solar conjunction by the NASA Infrared Telescope Facility, by JunoCam, and by amateur astronomers. It unfolded in essentially the same way as previous such outbreaks, leading to revival of the North Temperate Belt with a notably red component. The maturation of this belt was monitored at high resolution by JunoCam.

1. Introduction

Each of Jupiter's 3 major belts is subject to planetary-scale cycles in which a quiescent preparative phase with increased cloud cover is followed by a sudden vigorous outbreak of activity. In the North Temperate Belt (NTB), the most distinctive feature of its cycle is a sudden outbreak of several vertically extended convective plumes, very bright at all wavelengths from UV to near-IR, which travel at 165-175 m/s, the maximum speed of the planet's fastest jet at 23-24°N (NTBs jet) [1,2]. The plumes are typically followed by expanding chains of slower-moving dark spots and streaks on the jet, which merge to form a new NTB south component (NTB(S)) which turns an intense orange colour within a few months. We refer to these events as 'super-fast NTB outbreaks'; they have also been termed 'NTB Disturbances' [2] and 'NTB Revivals'. Outbreaks of this type occurred every 4.9 (± 0.2) years from 1970 to 1990 (assuming an unobserved event in 1985) [1]. Further super-fast outbreaks occurred in 2007 and 2012.

The NTBs jet at cloud-top level gradually accelerated over several years before the 2007 outbreak [2,3], while the NTB was whitened. This behaviour is in accord with Voyager observations, and with modelling [2,4]. Therefore, in early 2015, when the jet again had intermediate speed (Fig.1) and the belt had become visibly pale, a prediction was issued for another outbreak in late 2016 or early 2017 [5].

The event duly began during solar conjunction in autumn 2016, and was discovered by G.O. by IR imaging scheduled to coincide with Juno's perijove 2 on Oct.19. Fortuitously, Juno's 'public outreach' camera, JunoCam, had been taking distant low-resolution images of Jupiter every 30 minutes up to Oct.14, and the early stages of the outbreak could be discerned in these images. So, although Juno returned no science data at perijove 2, it was instrumental in recording the earliest stages of this outbreak. Ground-based imaging by several amateurs, in visible light and near-IR and the 0.89-micron methane band, then tracked the plumes until they disappeared around the start of November. The early stages of the outbreak are described with further details of the spot motions and with modelling in [6].

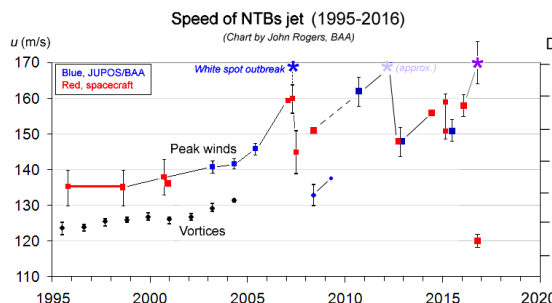


Figure 1. Chart of NTBs jet peak speed over recent decades.

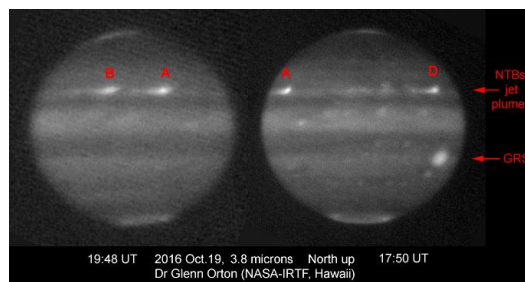


Figure 2. Discovery images of the NTB plumes, 2016 Oct.19 (from SpeX on the IRTF at 3.8 μ m, sensitive to gas absorption).

2. Methods

The methods for obtaining and analysing the early JunoCam, infrared, and amateur images are described in [6]. Subsequent JunoCam images were obtained as described [7] [& see separate abstract], thanks to members of the public voting for the so-called 'Big Red Stripe' target. Ground-based images were provided by the world-wide network of amateur observers who contribute to databases such as PVOL2, ALPO-Japan, and JunoCam. Maps were made from them by M.V. using WinJUPOS.

3. Results

The discovery images in mid-IR on Oct.19, taken from the NASA IRTF on Hawaii, revealed 3 brilliant plumes on the NTB jet (Fig.2), as well as numerous small 'hot spots' at 5 microns which are believed to correspond to visibly dark spots. JunoCam images from Oct.11-14 showed that the outbreak then contained 4 super-fast plumes, and was already widespread, with chains of dark bluish spots following the plumes. We measured the rapid speeds of the plumes and slower speeds of the dark spots, and estimated that the larger group of plumes and spots had appeared in mid-September, and the smaller group in early October.

The JunoCam measurements of plumes A and D connected up well with measurements from IRTF and amateur images over the following 2 weeks. Continuity of plumes B and C was less clear, as only one of them was observable after Oct.14. The mean speed of plumes A, C and D, from observations before and after Oct.14, was 170 (± 6) m/s. The speeds were typical, except that plume C was, marginally, the fastest ever recorded (~ 179 m/s).

Plumes A and D were both last seen when they caught up with the dark spots preceding them: plume D on Oct.28, and plume A on Oct.31.

At that time, the reviving NTB(S) consisted of very dark spots or streaks, starting to merge into a continuous belt. The NTB(S) reddened rapidly in late Nov., and remained outstandingly orange and almost featureless into spring, 2017. The NTB(N) was all turbulent in Nov-Dec., then became a well-defined, very dark grey belt in Jan., and even more regular from Feb. onwards. The NTB was essentially uniform in longitude, except for one turbulent sector of NTB(N) which probably persisted from 2015 and thus survived the NTBs jet outbreak.

JunoCam took close-up images of the maturing NTB at perijoves 3, 4 & 5, dramatically showing the complex texture of the reviving belt.

4. Conclusions

Given that only 3 previous NTB outbreaks were well observed, the present observations are a valuable confirmation of their stereotyped nature. The initial plumes were so far apart that they must have appeared in at least two locations independently, as has also been observed previously; and only in the 1975 outbreak were 4 plumes recorded, by amateur visual observers [1]. The JunoCam images of the maturing NTB revival will allow measurements of the evolving scale of the turbulence.

We cannot yet predict whether another such outbreak will take place 4-5 years after this one. This will become clearer over the coming year or two, according to whether the jet speed remains low or accelerates up towards super-fast speed again.

Acknowledgements

Some of this research was funded by NASA. A portion of this was distributed to the Jet Propulsion Laboratory, California Institute of Technology. We are grateful to all the contributing observers, especially P. Miles, A. Wesley, I. Miyazaki, T. Ashcraft, & J-L. Dauvergne.

References

- [1] Rogers JH (1995) *The Giant Planet Jupiter* (CUP).
- [2] Sanchez-Lavega A et al. (2008) 'Depth of a strong jovian jet from a planetary-scale disturbance driven by storms.' *Nature* 451, 437-440.
- [3] Rogers JH, Mettig H-J, and Peach D (2006). 'Renewed acceleration of the 24°N jet on Jupiter.' *Icarus* 184, 452-459.
- [4] Garcia-Melendo E, Sanchez-Lavega A & Dowling TE (2005) 'Jupiter's 24°N highest-speed jet: vertical structure deduced from nonlinear simulations of a large-amplitude natural disturbance.' *Icarus* 176, 272-282.
- [5] Rogers J (2015) 'A 3-year weather forecast for Jupiter: Prospects for Jupiter in 2015-2017.' http://www.britastro.org/jupiter/2014_15reports.htm [Report no.5].
- [6] Sánchez-Lavega A, Rogers JH, Orton GS, et al. (2017) 'A planetary-scale disturbance in the most intense Jovian atmospheric jet from JunoCam and ground-based observations.' *Geophys.Res.Lett.* (in press) doi: 10.1002/2017GL073421
- [7] Hansen CJ, Caplinger MA, Ingersoll A, Ravine MA, Jensen E, Bolton S & Orton G (2014). 'JunoCam: Juno's outreach camera.' *Space Sci. Rev.* doi:10.007/s11214-014-0079-x

Juno, The Cultural Connection

T. Clarke

Please make sure that your pdf conversion results in a document with a page size of 237 x 180 mm!

Abstract

After a 5-year journey and a billion miles cartwheeling through the vastness of space, the Juno spacecraft is in orbit about the planet Jupiter. With its suite of scientific instruments Juno scientists will catch a glimpse of the dawn of creation of our own solar system. Juno will address origins, asking for us all, “Who am I? Where do I come from?”

But Juno is more than a space laboratory to study the planet Jupiter. Juno embodies the history of humankind’s perception of the universe from Aristotle, Copernicus and Galileo, to the Juno spacecraft peering beneath the clouds of Jupiter. Juno embodies the literature of classical mythology and the timeless masterpieces of the Renaissance and Baroque periods in its very name. Juno carries to Jupiter small statuettes of the gods Jupiter and Juno and the scientist Galileo. Juno embodies cosmic visualization experiences through first ever movies of the moon occulting Earth and the Galilean satellites orbiting about Jupiter.

Juno embodies the stirring music of modern Greek composer Vangelis, the Orpheus of Juno, who provided the score for the movies of the moon occulting Earth and of the Galilean satellites orbiting Jupiter. Juno embodies down to Earth visualization experiences through trajectory models created of Juno’s passage through the Earth-moon system and Juno’s entire orbital mission at Jupiter. Juno is the embodiment of public engagement in its science in a fishbowl program.

Because Juno is the embodiment of this remarkable union of science and technology, history and literature, music and art, and visualization and public engagement, Juno is truly an ambassador to the universe of a New Renaissance.

This paper unveils the cultural dimension of the Juno mission to Jupiter.

Juno-UVS and Chandra Observations of Jupiter's Polar Auroral Emissions

G. R. Gladstone (1,2), J. A. Kammer (1), M. H. Versteeg (1), T. K. Greathouse (1), V. Hue (1), J.-C. Gérard (3), D. Grodent (3), B. Bonfond (3), C. Jackman (4), G. Branduardi-Raymont (5), R. P. Kraft (6), W. R. Dunn (5), S. J. Bolton (1), J. E. P. Connerney (7), S. M. Levin (8), B. H. Mauk (9), P. Valek (1,2), A. Adriani (10), W. S. Kurth (11), and G. S. Orton (8)

(1) Southwest Research Institute, San Antonio, TX, USA, (2) Department of Physics and Astronomy, University of Texas at San Antonio, San Antonio, TX, USA, (3) Université de Liège, Liège, Belgium, (4) University of Southampton, Southampton, UK (5) Mullard Space Science Laboratory, University College London, Holmbury St. Mary, UK, (6) Smithsonian Astrophysical Observatory, Cambridge, MA, USA (7) NASA Goddard Space Flight Center, Greenbelt, MD, USA, (8) Jet Propulsion Laboratory, Pasadena, CA, USA, (9) The Johns Hopkins University Applied Physics Laboratory, Laurel, MD, USA, (10) INAF-Istituto di Astrofisica e Planetologia Spaziali, Roma, Italy, (11) University of Iowa, Iowa City, IA, USA (rgladstone@swri.edu / Fax: 210-522-4520)

Abstract

The Juno spacecraft polar orbit provides an excellent platform for observing Jupiter's bright and transient polar auroral emissions [1]. These emissions occur as flares at far-ultraviolet (FUV) wavelengths [2], which have been associated with X-ray bursts [3]. During 2017, joint Juno-UVS and Chandra HRC-I observations are being executed during four Juno perijoves to further investigate these polar auroras.

1. Polar Emissions

Ultraviolet and X-ray observations of Jupiter's auroras have provided valuable insights into the fundamental processes of charged particle acceleration and the resulting currents in Jupiter's magnetosphere [4]. The cusp or active regions of Jupiter's polar auroras are the site of highly-variable X-ray, FUV, and thermal-IR auroral emissions. The northern hot spot is typically found near a system III longitude of 170° and latitude of 65° (easily seen from Earth), and the corresponding southern region is visible when conditions are favorable, as they are during the Juno mission when the sub-Earth latitude is as far south as it can be).

2. Juno-UVS and Chandra Support

Juno-UVS is an imaging spectrograph with a bandpass of $70 < \lambda < 205$ nm [5]. This wavelength range includes important far-ultraviolet (FUV) emissions from the H₂ bands and the H Lyman series which are produced in Jupiter's auroras, and also the absorption signatures of aurorally-produced hydrocarbons. A flat scan mirror situated near the

entrance is used to observe at up to $\pm 30^\circ$ perpendicular to the Juno spin plane. Tantalum surrounds the spectrograph assembly to shield the Juno-UVS MCP detector and its electronics from high-energy electrons. The purpose of Juno-UVS is to remotely sense Jupiter's auroral morphology and brightness to provide context for in situ measurements by Juno's particle instruments.

Using Chandra's HRC-I camera, we are monitoring auroral X-ray emissions from Jupiter when the cusp region is in a good location for simultaneous observations by Juno-UVS and Chandra. Half the observations are planned to focus the northern cusp and half on the southern cusp. Our primary goal is to study the morphology of the cusp region emissions, comparing simultaneous high-spatial resolution Chandra HRC-I observations with very-high spatial resolution Juno-UVS observations to test different physical theories of the source of the emissions.

During 2017, joint Juno-UVS and Chandra HRC-I observations are planned for PJ4, PJ5, PJ6, and PJ7, and the results of observations through PJ8 will be presented at EPSC.

3. Initial Results

Initial results for PJ4 are shown in Figs. 1-3, where transient southern polar FUV emissions decrease markedly in brightness during the same period as a large decrease in auroral X-ray brightness. Maps of the X-ray emissions will be compared with the FUV maps to investigate these polar auroras further.

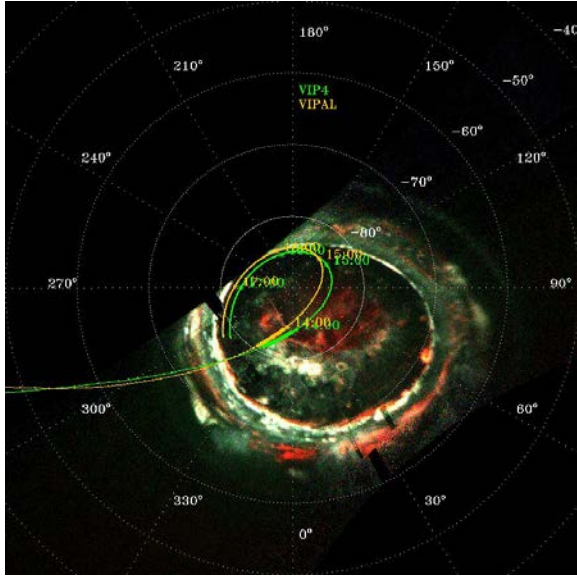


Figure 1: False color map of the southern aurora observed by Juno-UVS in during PJ4 on 2 February 2017 13:50-14:00. Red colors indicate high FUV color ratios. Juno magnetic footprints according to VIP4 and VIPAL are indicated by green and yellow lines, respectively, which are thicker for the 10-minute period when Juno-UVS data were taken.

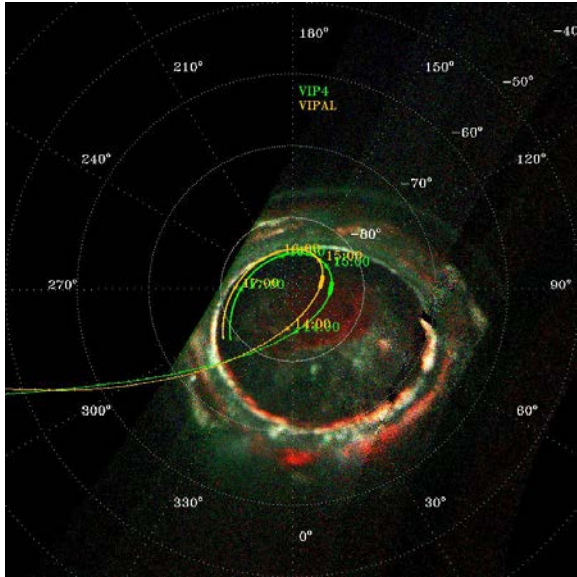


Figure 2: As in Fig. 1, but for 14:30-14:40. The polar emissions are distinctly fainter at this time than during the 40-minute earlier period of Fig. 1.

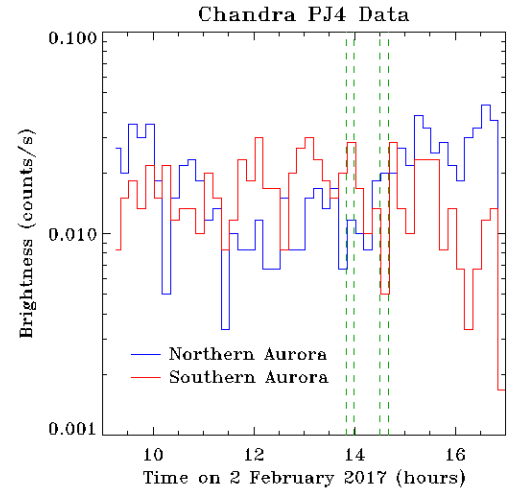


Figure 3: Histograms of X-ray count rates from the northern and southern auroras as observed by Chandra HRC-I during PJ4, corrected for one-way light time. The left and right pairs of vertical dashed green lines show the times presented in Figs. 1 and 2, respectively. Note the $\sim 6\times$ drop in X-ray brightness between these two periods, consistent with the drop in FUV brightness.

Acknowledgements

This research was funded by the National Aeronautics and Space Administration through the Juno Project.

References

- [1] Grodent, D.: A brief review of ultraviolet auroral emissions on giant planets, *Space Sci. Rev.*, Vol. 187, pp. 23-50, 2015.
- [2] Waite, J. H., Jr., et al.: An auroral flare at Jupiter, *Nature*, Vol. 410, pp. 787-789, 2001.
- [3] Elsner, R. F., et al.: Simultaneous Chandra X-Ray, Hubble Space Telescope Ultraviolet, and Ulysses radio observations of Jupiter's aurora, *J. Geophys. Res.*, Vol. 110, p. A01207, 2005.
- [4] Badman, S. V., et al.: Auroral processes at the giant planets: Energy deposition, emission mechanisms, morphology and spectra, *Space Sci. Rev.*, Vol. 187, pp. 99-179, 2015.
- [5] Gladstone, G. R., et al.: The Ultraviolet Spectrograph on NASA's Juno mission, *Space Sci. Rev.*, 2014.

Detection of Compact Baroclinic Waves in Jupiter's Deep Clouds at 5-microns from the VLT

L.N Fletcher (1), P. Donnelly (1), H. Melin (1), G.S. Orton (2), T.K. Greathouse (3), J.A. Sinclair (2), R.S. Giles (2), A.A. Simon (4), I. de Pater (5), M. Wong (5)

(1) Department of Physics and Astronomy, University of Leicester, UK (leigh.fletcher@le.ac.uk; Tel: +44 116 252 3585); (2) Jet Propulsion Laboratory, Pasadena, USA; (3) Southwest Research Institute, San Antonio, USA; (4) NASA Goddard Spaceflight Center, Maryland, USA; (5) University of California-Berkeley, USA.

Abstract

Hubble Space Telescope (HST) observations of Jupiter's North Equatorial Belt (NEB) in 2015 revealed the presence of a small-scale wave pattern interpreted as a baroclinic instability associated with the chain of cyclones on the northern edge of the NEB (near 16°N) [1]. The waves spanned 2-3° latitude, with a wavelength of approximately 1° longitude. Given that such disturbances are sensitive to atmospheric stratification, we employed the VISIR mid-infrared imager on the VLT [2] and the TEXES instrument on Gemini to diagnose the thermal conditions in this region [3]. Throughout 2016 and 2017 we employed VLT 'lucky imaging' at 5 μ m to reduce the effects of atmospheric seeing, stacking only the sharpest frames to yield global 5- μ m images with exquisite detail, providing spatial context to Juno's close perijove encounters. We report the first detection of the compact wave pattern at 5 μ m, indicating that this wave modulates aerosol opacity in the NEB at high pressures (2-3 bar), significantly deeper than expected from the HST imaging alone. The waves were observed west of a dark putatively-cyclonic vortex in December 2016 and January 2017, spanning a limited longitude range of ~50°. They were only visible in regions of relatively uniform 5- μ m emission. More turbulent regions of the NEB did not display similar features. Near-coincident HST observations also confirm the re-detection of this wave in localised regions, allowing us to compare the structure over a variety of altitudes. The ground-based data allow us to compare thermal and aerosol structures in regions with and without this compact wave pattern. Observations will be compared to those of Juno/JIRAM when available.

1. VLT/VISIR Observations

With the refurbishment of the VISIR instrument between 2012 and 2015, ESO now offers the capability for burst-mode imaging of bright targets at 5- μ m using an M-band filter. Burst mode allows us to

employ the 'lucky imaging' technique, selecting only the sharpest frames from a video sequence over ~2 minutes of observing time. This allows us to discard frames that are blurred by atmospheric seeing, resulting in the sharpest full-disc images of Jupiter ever obtained from Earth at 5 μ m. Images were reduced using a custom IDL pipeline and stacked using Autostakkert [4]. After a first proof-of-concept observation in February 2016, this burst mode observing is now employed at least once per Juno perijove to provide wide spatial context to the close-in imaging from the spacecraft, with data acquired in December, January, February and March, with more expected in May, July and September 2017.

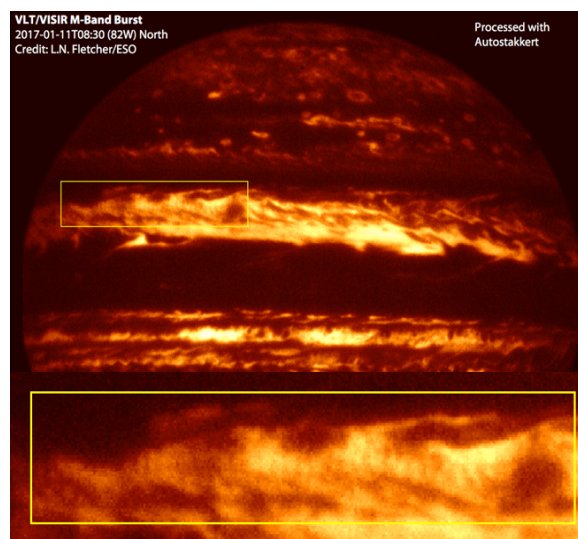


Figure 1 Example of 5- μ m VISIR imaging in January 2017, with the yellow box indicating the detection of the compact wave pattern.

Fig. 1 shows the identification of the compact wave pattern in one example of a 5- μ m image, confirming that this fine wave is modulating opacity at deep pressures. Observations in March 2017, along with polar projections of these maps, are shown in Fig. 2.

These do not show the compact wave, but reveal a chain of putatively cyclonic features at the northern edge of the NEB (remaining from the NEB expansion phase in 2015-16, [2]), and chaotic activity in the South Equatorial Belt (SEB) associated with a recent outbreak of moist-convective activity [5]. The polar projection also reveals an intensely bright band on the northern edge of Jupiter's North Temperate Belt (NTB(N)) following outbreak activity on the southern edge (NTBs) in October 2016 [6]. This narrow band was not visible in our February 2016 data, suggesting that it may have formed as a consequence of the NTBs outbreak. The polar projections show latitudinal contrasts in 5- μm emission, with a distinct change in character near 45°N and (tentatively) a band of higher opacity between 60°N and 70°N , on the edge of the polar domain imaged by Juno. The two hemispheres are asymmetric, with the south showing brighter emission between 35°S and poleward of 65°S . The cause of this long-lived asymmetry in 5- μm banding remains unclear.

2. Gemini/TEXES Observations

To further constrain the background environment in which these waves propagate, we moved the TEXES spectrograph from the 3-m IRTF to the 8-m diameter Gemini Observatory. Repeatedly scanning Jupiter's tropical domain over two nights in March 2017 has provided the highest-resolution mid-IR spectral map of Jupiter ever obtained. Eight spectral channels are used between 5-20 μm [3]. Fig. 3 shows a three-colour composite from just one channel near 8.6 μm , sensing temperatures, aerosols and PH_3 in the upper troposphere. These show spectral changes with longitude in the NEB, allowing us to deduce thermal and compositional contrasts in the regions hosting the

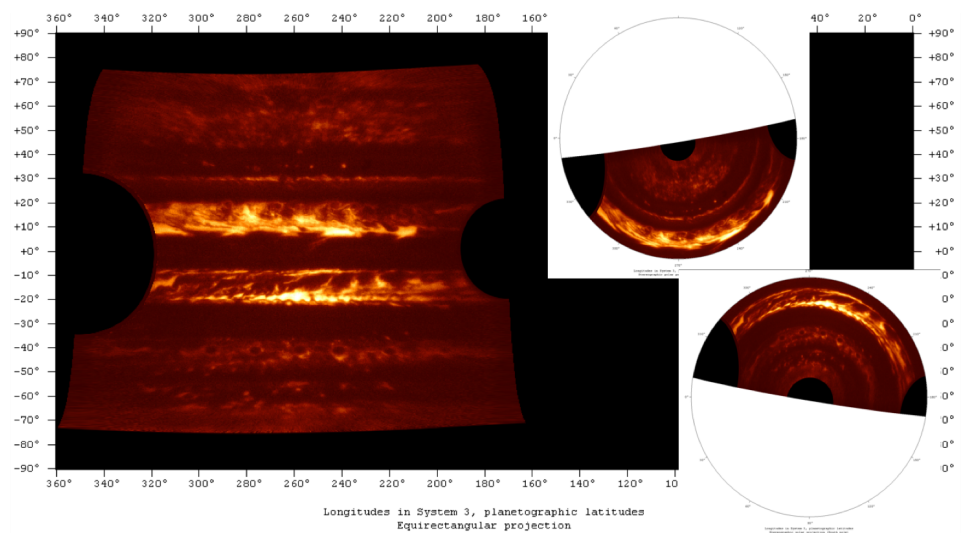


Figure 2 Maps of VISIR 5- μm observations on March 16, 2017, showing the turbulent NEB, the mid-SEB outbreak, and the bright NTB(N) band. Inset are polar projections of the north and south.

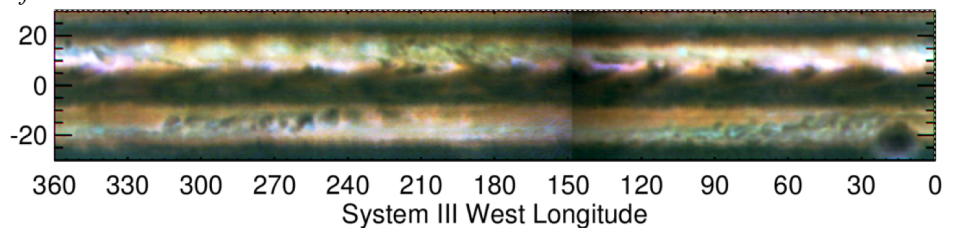


Figure 3 Three-colour map from one TEXES spectral channel near 8.6 μm (Mar 12-13, 2017), using absorptions of decreasing strength from red to green to blue.

compact wave train (as well as in the mid-SEB outbreak, clearly seen between 240°W and 300°W and possessing similar conditions to the turbulent wake of the Great Red Spot). Taken together, the VLT 5- μm images and the Gemini/TEXES spectroscopic maps will provide important constraints on temperatures, clouds, ammonia and phosphine in Jupiter's upper troposphere to support Juno.

Acknowledgements

LNF is supported by a Royal Society Research Fellowship and a European Research Council Consolidator Grant at the University of Leicester. The UK authors acknowledge the support of the Science and Technology Facilities Council (STFC).

References

- [1] Simon et al., 2015 (doi:10.1088/0004-637X/812/1/55)
- [2] Fletcher et al., 2017b, (doi: 10.1002/2017GL073383)
- [3] Fletcher et al., 2016, (doi: 0.1016/j.icarus.2016.06.008)
- [4] E. Kraaikamp, Autostakkert (www.autostakkert.com)
- [5] Fletcher et al., 2017a. (doi: 10.1002/2017GL073383)
- [6] Sanchez-Lavega et al., 2017, GRL, in press.

Observations of the Jupiter poles by the infrared spectral-imager JIRAM on board Juno

A. Adriani (1), A. Mura (1), M. L. Moriconi (2), F. Altieri (1), B.M. Dinelli (2), G. Sindoni (1), D. Turrini (1), G. Filacchione (1), A. Migliorini (1), F. Tosi (1), R. Noschese (1), A. Cicchetti (1), F. Fabiano (2,3), G. Piccioni (1), C. Plainaki (4), A. Olivieri (4), M. Amoroso (4), S. Bolton (5), S. Atreya (6), J. Lunine (7)
(1) INAF-Istituto di Astrofisica e Planetologia Spaziali, Roma, Italy (alberto.adriani@iaps.inaf.it), (2) CNR-Istituto di Scienze dell'Atmosfera e del Clima, Bologna e Roma, Italy, (3) Dipartimento di Fisica e Astronomia, Università di Bologna, (4) Agenzia Spaziale Italiana, Roma, Italy, (5) Southwest Research Institute, San Antonio, Texas, USA, (6) University of Michigan, Ann Arbor, Michigan, USA, (7) Cornell University, Ithaca, New York, USA

Abstract

The Juno polar orbit permitted JIRAM, the InfraRed Auroral Mapper [1], to observe the Jupiter poles with unprecedented resolution during the perijove passes PJ4 and PJ5. During PJ4 the coverage was complete while only partial during PJ5 due to the different attitude of the spacecraft. The images have been collected in the 4.5-5 μm wavelength range in several scans at different spatial resolutions varying from 14 km to 90 km, depending on the distance of the spacecraft from the planet.

JIRAM could identify clusters of circumpolar cyclones (CPCs) surrounding the polar cyclones, which appear to be off the geographical poles with significant differences between north and south. Also the number of CPCs is different in the north compared to the south. The CPCs are arranged in a quasi-octagonal shape in the north while in the south they are approximately distributed on the vertices of a pentagon centered on the polar cyclone.

On the basis of successive observation sequences it is possible to reconstruct the motion of the cyclones where the rotation speed can reach velocities of up to a few hundred kilometers per hour.

Comparison between PJ4 and PJ5 images permits the identification of the motion of the structures in the time elapsed between the two perijove passes, currently about 53 days.

Detailed results will be presented in this talk.

Acknowledgements

The project JIRAM is funded by the Italian Space Agency.

References

- [1] Adriani et al. (2014), JIRAM, the Jovian Infrared Auroral Mapper. *Space Sci. Rev.*, doi 10.1007/s11214-014-0094-y.

Jupiter Brightness Temperature Maps as derived from Juno/JIRAM data

F. Altieri (1), M. L. Moriconi (2), A. Mura (1), A. Adriani (1), G. Sindoni (1), A. Migliorini (1), G. Filacchione (1), B.M. Dinelli (2), F. Tosi (1), F. Fabiano (3), D. Turrini (1), R. Noschese (1), A. Cicchetti (1), G. Piccioni (1), C. Plainaki (4), A. Olivieri (4), S. Bolton (5), S. Atreya (6), J. Lunine (7)

(1) INAF-Istituto di Astrofisica e Planetologia Spaziali, Roma, Italy (francesca.altieri@iaps.inaf.it), (2) CNR-Istituto di Scienze dell'Atmosfera e del Clima, Bologna e Roma, Italy, (3) Dipartimento di Fisica e Astronomia, Università di Bologna, Italy (4) Agenzia Spaziale Italiana, Roma, Italy, (5) Southwest Research Institute, San Antonio, Texas, USA, (6) University of Michigan, Ann Arbor, Michigan, USA, (7) Cornell University, Ithaca, New York, USA

Abstract

JIRAM is the InfraRed Auroral Mapper on board the Juno mission arrived at Jupiter on July 4 2016. The instrument is composed by two imager channels (L and M), and a spectrometer channel (SPE) [1]. L channel is centered at 3.455 μm with a 290 nm bandwidth, devoted to the auroral emission mapping. M channel is centered is at 4.780 μm with a 480 nm bandwidth and can sound the thermal emission from the deeper atmosphere of the planet. Their Field of View (FOV) is of the order of $1.75^\circ \times 5.94^\circ$ (128×432 pixels corresponding to the along and across track directions), with an Instantaneous Field of View (IFOV) of $250 \times 250 \mu\text{rad}$. The spectrometer channel covers the 2.0–5.0 μm range with a spectral sampling of about 8.99 nm/band. It is able to realize co-located imaging spectroscopy in the M-filter channel FOV by using a slit 256 samples-wide with a FOV of 3.52° and an IFOV of $250 \mu\text{rad}$.

In this work we derive Jupiter brightness temperature maps from both the M channel (4.780 μm) and the spectrometer (4.6-5.0 μm range), compare their distribution and discuss the results.

Acknowledgements

The project JIRAM is funded by the Italian Space Agency.

References

[1] Adriani et al. (2014), JIRAM, the Jovian Infrared Auroral Mapper. Space Sci. Rev., doi 10.1007/s11214-014-0094-y.

Characterising Jupiter's Temperatures, Aerosols and Ammonia via VLT/VISIR Spatial Mapping 2016-17

P. T. Donnelly (1), L.N. Fletcher (1), G.S. Orton (2), H. Melin (1)

(1) Dept. of Physics and Astronomy, University of Leicester, UK, (2) Jet Propulsion Laboratory, California Institute of Technology, USA

Abstract

The VISIR mid-IR imager (5-25 μm) on the Very Large Telescope (VLT) has been providing infrared spatial and temporal support for NASA's Juno spacecraft, constraining atmospheric thermal conditions in the upper troposphere (100-700 mbar) and stratosphere (1-10 mbar). Our pre-Juno-arrival dataset (January-August 2016) demonstrated that Jupiter's North Equatorial Belt (NEB) began a northward expansion in late 2015, consistent with the 3-5 year cycle of NEB activity. VISIR detected two new thermal waves during this period; an upper tropospheric wave in the mid-NEB and a stratospheric wave centred on the eastward jet at 23.9°N. The latter was quasi-stationary and both waves are morphologically similar to those observed during the 2000 expansion event by Cassini. We now extend this analysis to coincide with Juno's perijove encounters, once every 53.5 days. We report (i) the continued existence of the mid-NEB wave; (ii) evolution of Jupiter's North Temperate Belt (NTB) following the October 2016 outbreak; and (iii) complex thermal variability associated with a mid-SEB outbreak during 2017. We discuss zonally-averaged temperatures, aerosols and ammonia distributions derived from VLT data (taking centre-to-limb variations into account), comparing the upper-tropospheric aerosols and ammonia to the findings of Juno's near-infrared and microwave observations.

1. Introduction: Variability

The VISIR observations during the Juno epoch contribute to a time-series of VLT imaging that now spans a full Jovian year (2006-2017). Observations at eight narrow-band channels sense stratospheric temperatures (7.9 μm), tropospheric temperature (13.0, 17.6, 18.6, 19.5 μm), aerosols (8.6 μm) and ammonia (10.7 and 12.3 μm), and are inverted via our optimal estimation retrieval algorithm, NEMESIS [1]. This long time-series has allowed us to investigate thermal variability associated with fades and revivals of the South Equatorial Belt [2, 3], and the recent expansion of the NEB [4]. In this paper, we report the findings

of the NEB and the activity at other latitudes (the NTB and SEB) during the Juno epoch, and use the data to provide cloud-top estimates of temperatures, ammonia and aerosols to compare to Juno's perijove observations.

2. Thermal Field in 2017

The 2015/16 NEB expansion was unusual. Previous NEB expansions have encircled the entire globe, but this one stalled after February and began to regress from both ends. At this point, it spanned 140° of longitude and was 4° further northwards than the non-expanded sector. VLT/VISIR images in March 2016 suggest northern edge beginning to grow dim at 8.6 μm (a re-establishment of the aerosol opacity over the NTropZ). By the time of Juno's arrival, the expanded sector had returned to normal and the 8.6 μm -dark NTropZ again extended fully around the planet.

During the expansion, two waves were identified: a mid-NEB thermal wave that appeared quasi-stationary and showed an anticorrelation between temperatures and upper tropospheric haze reflectivity; and a stratospheric wave from 20-30°N. Both are similar to waves observed during previous expansion cycles and both persisted after Juno's arrival. The mid-NEB wave remains present today (Fig. 1).

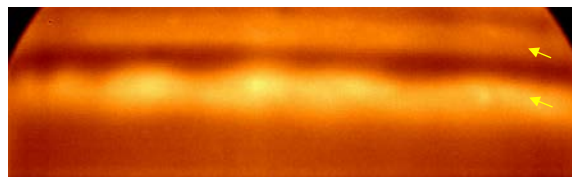


Figure 1: VLT/VISIR 17.65- μm observation for 11 Jan 2017, probing upper-tropospheric (150mbar) temperatures showing persistent wave activity over the NEB region. NEB and NTB shown by yellow arrows.

We also report on variations at Jupiter's northern temperate latitudes (specifically the NTB), where four plumes erupted in October 2016 and may have altered temperatures and composition in this region. Our

inversions of VISIR data will produce zonally-averaged temperatures in the NTB before and after the plume outbreak, allowing comparison of these conditions. Furthermore, the VISIR observations in 2017 have continued to track an outbreak of moist convective activity in the mid-SEB: we will describe the processes at work shaping this complex region (Fig. 2).

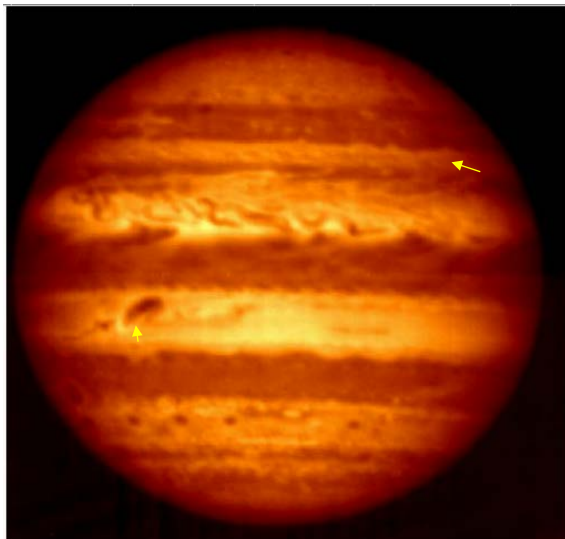


Figure 2: VLT/VISIR 8.6- μ m observation for 10 Jan 2017, probing cloud-tops (650mbar). The NTB and the outbreak in the mid-SEB are denoted by the yellow arrows.

3. Equatorial Ammonia – Abundances and Distribution

Recent findings from Juno suggest that there is a peak in ammonia at the equator, with the region over the NEB also being more depleted than SEB. This is consistent with previous thermal-IR spectroscopic analyses [5, 6], which suggest strong equatorial upwelling, but have confirmed that this zone of elevated ammonia persists to great depths below the clouds. By inverting zonal-mean VISIR observations, taking into account their dependence on emission angle, we will assess whether VISIR imaging alone is sensitive to this equatorial ammonia maximum, allowing us to map its variation with longitude and with time through the full decade-long dataset.

Summary and Conclusions

VISIR thermal imaging provides a regular source of information on the temperatures, aerosols and ammonia distributions associated with the phenomena studied by Juno. They also place the Juno epoch into the wider context of Jovian variability over a full ~ 12 year orbit. We expect also to have observations covering perijoves 6, 7 and possibly 8. Future work will include the use of N-band spectroscopy to further constrain chemical abundances, and direct comparisons with deep structures observed at microwave wavelengths.

Acknowledgements

PTD was supported by an STFC studentship; Fletcher was supported by a Royal Society Research Fellowship at the University of Leicester. The UK authors acknowledge the support of the Science and Technology Facilities Council (STFC).

References

- [1] Irwin, P., Teanby, N., de Kok, R., Fletcher, L. N., Howett, C., Tsang, C., Wilson, C., Calcutt, S., Nixon, C., Parrish, P., The NEMESIS planetary atmosphere radiative transfer and retrieval tool, *Journal of Quantitative Spectroscopy and Radiative Transfer*, 109(6), 461 1136–1150, 2008.
- [2] Fletcher, L. N., Orton, G. S., Rogers, J. H., Simon-Miller, A. A., de Pater, I., Wong, M. H., Mousis, O., Irwin, P. G. J., Jacquesson, M., Yanamandra-Fisher, P. A., Jovian temperature and cloud variability during the 2009-2010 fade of the South Equatorial Belt, *Icarus*, 213, 564–580, 2011.
- [3] Fletcher, L.N., Orton, G.S., Rogers, J.H., Giles, R.S., Payne, A.V., Irwin, P.G.J., Vedovato, M., Moist Convection and the 2010-2011 Revival of Jupiter’s South Equatorial Belt. *Icarus* 286, 94–117, 2017a.
- [4] Fletcher, L. N., Donnelly, P. T., Orton, G. S., Sinclair, J. A., Melin, H., Rogers, J. H., Greathouse, T.K., Kasaba, Y., Fujiyoshi, T., Sato, T.M., Fernandes, J., Irwin, P.G.J., Giles, R.S., Jupiter’s North Equatorial Belt expansion and thermal wave activity ahead of Juno’s arrival, *Geophys. Res. Lett.*, 44, 1–9, 2017b.
- [5] Achterberg, R. K., Conrath, B., Gierasch, P. J., Cassini CIRS retrievals of ammonia in Jupiter’s upper troposphere, *Icarus*, 182, 169-180, 2006.

[6] Fletcher, L. N., Greathouse, T.K, Orton, G.S., Sinclair, J. A., Giles, R. S., Irwin, P. G. J, Encrenaz, T., Mid-infrared mapping of Jupiter's temperatures, aerosol opacity and chemical distributions with IRTF/TEXES, *Icarus*, 278, 128–161, 2016.

Jupiter gravity field from the Juno mission first year of data

D. Serra (1), W.M. Folkner (2), L. Iess (3), J. D. Anderson (4), S. W. Asmar (2), D. R. Buccino (2), D. Durante (3), L. Gomez Casajus (5), M. Gregnanin (3), A. Milani (1), M. Parisi (2), G. Tommei (1), P. Tortora (5), M. Zannoni (5)

- (1) University of Pisa, Department of Mathematics, Pisa, Italy (dserra@mail.dm.unipi.it)
- (2) Jet Propulsion Laboratory, California Institute of Technology, Pasadena (CA), USA
- (3) Università La Sapienza, DIMA, Roma, Italy
- (4) Southwest Research Institute, San Antonio (TX), USA
- (5) University of Bologna, Dipartimento di Ingegneria Industriale, Forlì, Italy

Between its arrival at Jupiter, on July 4th, 2016 and September 1st, 2017, the Juno spacecraft has orbited the giant planet and performed eight close approaches at altitudes between 3500 and 4000 km above the cloud level. Three passes were dedicated to the determination of Jupiter's gravity field. The Deep Space Network (DSN) tracked the orbiter using a coherent, two-way radio tracking system at X-band (7.2-8.4 GHz) and - for perijove passes dedicated to gravity - at Ka-band (34.4-32.1 GHz), collecting very accurate measurements of the spacecraft range-rate. The goals of the gravity science investigation are to determine the zonal coefficients of the gravity field and the precession rate that will constrain interior structure models, to measure the response of Jupiter characterized by the k_2 Love number, and to determine the depth of deep zonal flows in Jupiter's atmosphere.

Doppler data were first calibrated to remove the media effects, namely the Earth troposphere and ionosphere, and, where possible, the solar and interplanetary plasma and the Io plasma torus. Then they were combined using a multi-arc strategy to obtain the best determination of Jupiter gravity field. The data analysis was performed using two different orbit determination and parameter estimation codes: NASA/JPL's MONTE and University of Pisa's ORBIT14. We present and compare the gravity solutions computed using the two codes and analyze the improvement over the previous solutions.

Characterization of the ovals in Jupiter's atmosphere using the first data by Juno/JIRAM instrument

G. Sindoni (1), A. Adriani (1), A. Mura (1), M.L. Moriconi (1,2), B.M. Dinelli (2), G. Filacchione (1), F. Tosi (1), G. Piccioni (1), A. Migliorini (1), F. Altieri (1), F. Fabiano (12,2), D. Turrini (1,13), R. Noschese (1), A. Cicchetti (1), S. Stefani (1), S.J. Bolton (3), J.E.P. Connerney (4), S.K. Atreya (5), F. Bagenal (6), C. Hansen (7), A. Ingersoll (8), M. Janssen (9), S.M. Levin (9), J.I. Lunine (10), G. Orton (9), C. Plainaki (11), A. Olivieri (11) and M. Amoroso (11).

- (1) Institute for Space Astrophysics and Planetology (IAPS-INAF), Rome, Italy (giuseppe.sindoni@iaps.inaf.it)
- (2) Institute of Atmospheric Sciences and Climate (ISAC-CNR), Bologna, Italy
- (3) Southwest Research Institute, San Antonio, Texas, USA
- (4) NASA Goddard Space Flight Center, Greenbelt, Maryland, USA
- (5) University of Michigan, Ann Arbor, Michigan, USA
- (6) University of Colorado, Boulder, Colorado, USA
- (7) Planetary Science Institute, Tucson, Arizona, USA
- (8) California Institute of Technology, Pasadena, California, USA
- (9) Jet Propulsion Laboratory, Pasadena, California, USA
- (10) Cornell University, Ithaca, New York, USA
- (11) Italian Space Agency (ASI), Rome, Italy
- (12) Dipartimento di Fisica e Astronomia, Università di Bologna, Italy
- (13) Departamento de Física, Universidad de Atacama, Copiapu 485, Copiapu, Chile

Abstract

Since the first orbits, the Jovian InfraRed Auroral Mapper (JIRAM) aboard the NASA/Juno spacecraft observed several oval vortices in the Jupiter's atmosphere with the highest spatial resolution achieved so far from space-borne infrared instruments. In particular, JIRAM highlighted a line of closely spaced oval features in Jupiter's southern hemisphere, between 30°S and 45°S (Fig. 1), as well as other persistent vortices in the northern hemisphere. The longitudinal region between 120°W and 60°W in System III coordinates covers the three ovals having higher contrast at 5 μ m. Using the JIRAM's full spectral capability in the range 2.4-3 μ m, which is sensitive to changes in high tropospheric clouds and in stratospheric hazes, as well as to gaseous ammonia, together with a Bayesian data inversion approach we retrieved maps of column densities and altitudes for an NH₃ cloud and a photochemical haze. The deep well-mixed volume mixing ratio and the relative humidity for gaseous ammonia were also retrieved. Our results suggest different vortex activity for the studied ovals. Vertical atmospheric dynamics together with considerations about the ammonia condensation could explain our maps providing evidence of cyclonic and anticyclonic structures.

1. Introduction

The white ovals, together with the Great Red Spot (GRS), are the most prominent features in the Jupiter's atmosphere. They were first observed by ground-based measurements [5], then in more detail during the flybys of Jupiter carried out by the NASA Voyager probes in 1979 and during the extensive in-system tour performed by the NASA Galileo spacecraft in 1995-2003. These ovals are in a stable configuration known as a "Karman vortex street", where anticyclones are staggered with cyclones [8].

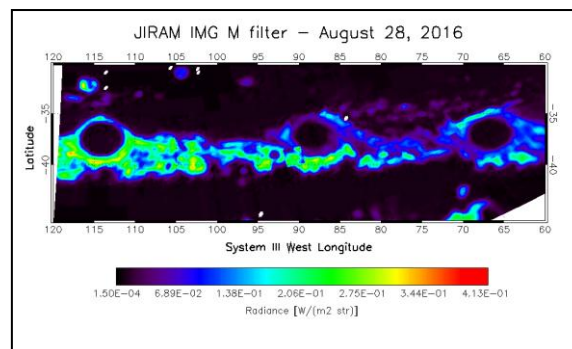


Figure 1: M-filter single image acquired by JIRAM Imager on 28th August 2016, where the three main ovals are clearly visible in the southern hemisphere of Jupiter. Image credits: [7].

The current understanding of the cloud structure in Jupiter's atmosphere is mainly related to theoretical

models based on the thermochemical equilibrium models [9, 2]. They predict an ammonia ice layer at about 700 mbar, an ammonium hydrosulfide cloud layer at about 2 bars and a water cloud layer with a base near 6 bars, if the N, S and O elemental abundances are 3x solar. Moreover, observations from the ground and space in the visible, near and thermal infrared provided important information about the aerosol composition of the planet [10, 11]

2. Instrument and Data Set

The JIRAM instrument, aboard the NASA/Juno spacecraft, is composed of an infrared imager (IMG) and a spectrometer (SPE) in the 2-5 μm range [1], sharing a common optical head. The imager is further split in two spectral channels: L-filter, centered at 3.45 μm with a 290 nm bandwidth, and M-filter, centered at 4.78 μm with a 480 nm bandwidth. In this work we used the M-filter of the IMG for the context and the SPE for the characterization analysis. Data we used were acquired during the first orbits of Juno.

3. Method

The retrieval of the atmospheric composition exploits the data inversion technique with the Bayesian approach [6]. It uses the Gauss-Newton iterative procedure to minimize the cost function.

The synthetic spectrum takes into account the multiple scattering, both by molecules and particles, and it is computed using a plane-parallel approximation [4]. Finally, the convergence criterion takes into account the χ^2 minimization.

The *a priori* knowledge of Jupiter's atmosphere is based on the model suggested by [3] and [7].

4. Conclusions and Future Work

The JIRAM measurements acquired during the first orbit of Juno around Jupiter highlighted the presence of several ovals. The preliminary analysis we performed on the three ovals (Oval#1, Oval#2 and Oval#3) showing the higher contrast in the M band (around 5 μm) using the JIRAM's full spectral capability in the range 2.4-3 μm allowed to infer about their dynamic nature. Indeed, the application of a data inversion algorithm based on a Bayesian approach provided information about the atmospheric structure inside and outside the oval vortices. As a result of our retrieval we produced maps for the column densities and the altitudes of a tholin-coated

NH_3 cloud and of a photochemical haze. Moreover, we mapped also the gaseous ammonia deep mixing ratio (below the expected saturation level) and its relative "humidity".

The results here reported are the first obtained from JIRAM observations and therefore should be regarded as preliminary. Simultaneous analysis of solar and thermal dominated spectral range, as well as the extension to other interesting atmospheric features, could provide important insights into the cloud structure and the gaseous content of Jupiter's atmosphere.

Acknowledgements

The JIRAM project is founded by the Italian Space Agency (ASI). In particular this work has been developed under the agreement n. 2016-23-H.0. The computational resources used in this research have been supplied by INAF-IAPS through the projects "HPP - High Performance Planetology" and "DataWell".

References

- [1] Adriani, A., et al. (2014). Space Sci. Rev., DOI 10.1007/s11214-014-0094-y.
- [2] Atreya S.K., et al. (1999). Planet. Space Sci., 47, 1243-62. doi:10.1016/S0032-0633(99)00047-1.
- [3] Grassi, D., et al. (2010). Planet Space Sci, 58, 1265-1278, doi:10.1016/j.pss.2010.05.003.
- [4] Ignatiev, N. I. et al., (2005). Planet. Space Sci., 53:1035-1042.
- [5] Peek, B.M., (1958). The Planet Jupiter. Faber and Faber, London.
- [6] Rodgers, C. D., 2000, Inverse Methods for Atmospheric Sounding. World Scientific.
- [7] Sindoni, G., et al., (2017). Geophys. Res. Lett., 44, doi:10.1002/2017GL072940.
- [8] Youssef, A., Marcus, P.S., (2003). Icarus 162, 74-93.
- [9] Weidenschilling, S., J., and Lewis, J., S., (1973). Icarus 20, 465-476. doi: 10.1016/0019-1035(73)90019-5.
- [10] West, R.A., Strobel, D.F., Tomasko, M.G., (1986). Icarus 65, 161-217.
- [11] West, R.A., et al., (2004). Cambridge Univ. Press, Cambridge, pp. 79-104.

Juno JADE observations at Jupiter

P. W. Valek (1,2), F. Allegrini (1,2), F. Bagenal (3), S. Bolton (1), J. Connerney (4), R. W. Ebert (1), G. R. Gladstone (1,2), T. K. Kim (2,1), W. S. Kurth (5), S. Levin (6), P. Louarn (7), B. Mauk (8), D. J. McComas (9,1), C. Pollock (10), M. Reno (11), J. R. Szalay (1), M. F. Thomsen (12), R. J. Wilson (3), J. L. Zink (2,1)
(1). Southwest Research Institute, San Antonio, Texas, USA, (2). University of Texas at San Antonio, San Antonio, Texas, USA (3). Laboratory for Atmospheric and Space Physics, University of Colorado, Boulder, Colorado, USA (4). NASA Goddard Space Flight Center, Greenbelt, Maryland, USA (5). University of Iowa, Iowa City, Iowa, USA (6). Jet Propulsion Laboratory, Pasadena, California, USA (7). Institut de Recherche en Astrophysique et Planétologie (IRAP), Toulouse, France (8). The Johns Hopkins University Applied Physics Laboratory, Laurel, Maryland, USA (9). Princeton University, Princeton, New Jersey, USA (10). University of Alaska Fairbanks, Geophysical Institute, Fairbanks AK, USA (11). Austin Mission Consulting, Austin, Texas, USA (12). Planetary Science Institute, Tucson, Arizona, USA

Abstract

Since the crossing of the Jovian bow shock on 24 June 2016 the Juno mission has performed measurements of the plasma environment across the Jovian magnetosphere. In situ measurements of the plasma environment are performed by the Jovian Auroral Distributions Experiment (JADE) [4]. JADE measures the plasma using two nearly identical electron sensors and an ion sensor. The electron sensors (JADE-E) measure the electron distribution in the range of 100 eV to 100 keV. The un-deflected Field-of-View (FOV) of JADE-E is the spin plane of the spacecraft; approximately the plane which includes the spacecraft velocity direction and the local magnetic field. Around closest approach the JADE-E sensors use electrostatic deflection to track the local magnetic field direction in order to measure the pitch angle distribution with nearly 1 second time resolution. The JADE ion sensor (JADE-I) measures the energy per charge and time of flight (TOF) of incident ions to observe the composition-separated ion distributions. The JADE-I sensor measures the energy per charge in the range of 10 eV / q to 50 keV / q for ions with masses < 64 amu / q. Using the spacecraft spin to sweep its FOV, JADE-I measures a full 4Pi ion distribution function every 30 seconds.

The large orbit – apojove ~ 110 R_J with a 53.4 day period – allows the Juno spacecraft to periodically cross through the magnetopause into the magnetosheath. This is observed in JADE as the plasma changes from a shocked solar wind in the sheath with anti-sunward flows to co-rotating magnetospheric plasma with sunward flow (at the

dawn flank) [2, 5]. We present observations of crossings of the magnetopause, observed with both the JADE-E and JADE-I sensors.

As the spacecraft travels inward toward the planet, JADE samples the plasma of the outer, middle, and inner magnetosphere. The polar orbit of Juno permits the direct sampling of both the lobes in addition to a large number of plasma sheet crossings each orbit. The JADE observations of the larger magnetospheric structure are presented here.

During times when Juno crosses the auroral regions, JADE-E found that the core of the energy distribution is generally within this energy range, going from about 100 eV, when Juno is on field lines that are connected to the inner plasmasheet, to several keVs, when Juno is connected to the outer plasmasheet, and to tens of keVs, when Juno is over the polar regions. JADE has observed upward electron beams and upward loss cones, both in the north and south auroral regions, and downward electron beams in the south. Some of the beams are of short duration (< 1 s) implying that the magnetosphere has a very fine spatial and/or temporal structure near the auroral regions [1]. Joint observations with the WAVES instrument have demonstrated that the observed loss cone distributions provide sufficient growth rates to drive the cyclotron maser instability [3].

The high velocity of the Juno spacecraft near perijove (~50 km/s) allows observations of very low energy ions in the spacecraft ram direction, down to below 1 eV/q. During the perijove passes when the

spacecraft is at sub-auroral latitudes the ion observations show two populations. The first appears to be of Iogenic origin based on its composition and velocity distribution [6]. The second population appears to come directly from Jupiter itself. This population consists of low energy, light ions, largely consisting of protons. The ions have energies below 100 eV in the spacecraft frame, and extend down to the bottom of the JADE measurement range. In this paper we will present observations of the ions in the sub-auroral regions and below an altitude of 1 R_J.

dawn flank of Jupiter's magnetosphere: Juno arrives at Jupiter. *Geophys Res Lett*, 2017. In this issue.

[6] J. R. Szalay, F. Allegrini, F. Bagenal, S. J. Bolton, G. Clark, J. E. P. Connerney, L. Dougherty, R. W. Ebert, D. J. Gershman, W. S. Kurth, S. Levin, P. Louarn, B. H. Mauk, D. J. McComas, C. Paranicas, D. A. Ranquist, M. Reno, M. F. Thomsen, P. W. Valek, S. Weidner, and R. J. Wilson. Plasma measurements in the jovian polar region with Juno/JADE. *Geophys Res Lett*, 2017. Under Review.

References

[1] F. Allegrini, F. Bagenal, S. J. Bolton, J. E. P. Connerney, G. Clark, R. W. Ebert, T. K. Kim, W. S. Kurth, S. Levin, P. Louarn, B. H. Mauk, D. J. McComas, C. J. Pollock, D. A. Ranquist, M. Reno, J. R. Szalay, M. F. Thomsen, P. W. Valek, S. Weidner, P. Wilson, and J. L. Zink. Electron beams and loss cones in the auroral regions of Jupiter. *Geophys Res Lett*, 44, 2017. Under Review.

[2] R. W. Ebert, F. Allegrini, F. Bagenal, S. J. Bolton, J. E. P. Connerney, G. Clark, G. A. DiBraccio, D. J. Gershman, W. S. Kurth, S. Levin, P. Louarn, B. H. Mauk, D. J. McComas, M. Reno, J. R. Szalay, M. F. Thomsen, P. W. Valek, S. Weidner, and R. J. Wilson. Accelerated flows at Jupiter's magnetopause: Evidence of magnetic reconnection along the dawn flank. *Geophys Res Lett*, 2017. in press.

[3] P. Louarn, F. Allegrini, D. J. McComas, P. W. Valek, W. S. Kurth, N. Andre, F. Bagenal, S. J. Bolton, J. E. P. Connerney, R. W. Ebert, M. Imai, S. Levin, J. R. Szalay, S. Weidner, R. J. Wilson, and J. L. Zink. Generation of the jovian hectometric radiation: first lessons from Juno. *Geophys Res Lett*, 2017. Accepted.

[4] D. J. McComas, N. Alexander, F. Allegrini, B. Bagenal, C. Beebe, G. Clark, F. Crary, M. I. Desai, A. De Los Santos, D. Demkee, J. Dickinson, D. Everett, T. Finley, A. Gribanova, R. Hill, J. Johnson, C. Kofoed, C. Loeffler, P. Louarn, M. Maple, W. Mills, C. Pollock, M. Reno, B. Rodriguez, J. Rouzard, D. Santos-Costa, P. Valek, S. Weidner, P. Wilson, R. J. Wilson, and D. White. The Jovian Auroral Distributions Experiment (JADE) on the Juno mission to Jupiter. *Space Sci. Rev.*, pages 1–97, 2013.

[5] D. J. McComas, J. R. Szalay, F. Allegrini, F. Bagenal, S. Bolton, J. Connerney, R. W. Ebert, G. R. Gladstone, W. S. Kurth, S. Levin, P. Louarn, B. H. Mauk, C. J. Pollock, M. Reno, M. F. Thomsen, P. W. Valek, S. Weidner, and R. J. Wilson. Plasma environment at the

Initial results for the depth of the winds on Jupiter as inferred from the Juno gravity measurements

E. Galanti and Y. Kaspi

Department of Earth and Planetary Sciences, Weizmann Institute of Science, Rehovot, Israel

Abstract

One of the primary goals of the Juno mission, now in orbit around Jupiter and performing close flybys of the planet, is to obtain a high precision gravity spectrum of the planet. Such data can be used to estimate the depth of Jupiter's observed cloud-level wind, and decipher the possible internal flows within the planet. Here we present the initial results from these gravity measurements which allow calculation of the depth and vertical profile of the observed zonal flows. We use a hierarchy of models including a layered Concentric Maclaurin Spheroid model for determining the static component of the gravity spectrum, and an analysis of the geostrophic balance for inferring the dynamical contribution to the gravity spectrum. In order to invert the gravity measurements into flow fields we use an adjoint based inverse model. The model is constructed to be as general as possible, allowing for both cloud-level wind extending inward, and a decoupled deep flow that is constructed to produce cylindrical structures with variable width and magnitude, or can even be set to be completely general. In light of the Juno gravity measurement first results, we discuss the Juno gravity experiment and the implications regarding Jupiter's differential rotation and atmospheric flows. Particularly we focus on the odd gravity moments, which reflect asymmetries between the northern and southern hemispheres and therefore are a pure signature of the dynamics with no contribution from the static planet. We also discuss the contribution of the flow to the even harmonics and its implications to the study of Jupiter's density structure and shape.

Juno/JEDI observations of energetic particles in Jupiter's polar magnetosphere

D. K. Haggerty (1), B. H. Mauk (1), C. Paranicas (1), G. Clark (1), P. Kollmann (1), A. M. Rymer (1), S. J. Bolton (2), J. E. P. Connerney (3), S. M. Levin (4), and T. E. Cravens (5)

(1) The Johns Hopkins University Applied Physics Laboratory, Laurel, MD United States (dennis.haggerty@jhuapl.edu)

(2) Southwest Research Institute, San Antonio, TX, United States

(3) NASA Goddard Space Flight Center, Greenbelt, MD, United States

(4) Jet Propulsion Laboratory, Pasadena, CA, United States

(5) The University of Kansas, Lawrence, KS, United States

Abstract

The Juno spacecraft's polar orbit provides an exceptional opportunity to study the high latitude magnetosphere in the largest and most dynamic auroral region in the solar system. The Jupiter Energetic particle Detector Instruments (JEDI) have SSD telescopes with multiple look directions and additional time-of-flight capabilities to measure ions and electrons from ~ 6 keV to ~20 MeV. These instruments resolve major ion species from ~30 keV/n, with coarser mass resolution for lower energy ions. JEDI instruments observed energetic heavy ions up to 20 MeV precipitating into the auroral regions during the first few Juno perijoves, with the intensity and spatial locations varying from one pass to the next. Precipitating energetic heavy ions are believed to be the source population for Jupiter's x-ray aurora. We report on the new observations of precipitating energetic heavy ions in the Jovian auroral regions. We will also compare and contrast the observations from each of the auroral passes.

Juno's Magnetometer Investigation: Early Results

J. E. P. Connerney (1,2), R. J. Oliverson (2), J. R. Espley (2), D. J. Gershman (2,3), J. R. Gruesbeck (2,3), S. Kotsiaros (2,4), G. A. DiBraccio (1,4), J. L. Joergensen (5), P. S. Joergensen (5), J. M. G. Merayo (5), T. Denver (5), M. Benn (5), J. B. Bjarno (5), A. Malinnikova (5), J. Bloxham (6), K. M. Moore (6), S. J. Bolton (7), S. M. Levin (8)
 (1) Space Research Corporation, Annapolis, MD, USA, (2) NASA Goddard Space Flight Center, Greenbelt, MD, USA, (3) University of Maryland, College Park, MD, USA, (4) Universities Space Research Association, Columbia, MD, USA, (5) Technical University of Denmark (DTU), Lyngby, Denmark, (6) Harvard University, Cambridge, MA, USA, (7) Southwest Research Institute, San Antonio, TX, USA, (8) Jet Propulsion Laboratory, Pasadena, CA, USA, (jack.connerney@nasa.gov)

Abstract

After nearly 5 years in space, the Juno spacecraft entered polar orbit about Jupiter on July 5 (UTC), 2016, in search of clues to the planet's formation and evolution. Juno probes the deep interior with measurements of Jupiter's magnetic and gravitational potential fields, and peers beneath the visible clouds at microwave frequencies to characterize water and ammonia abundance to depths of ~ 1000 atmospheres.

Juno's baseline mission plan [6] was designed, in part, to wrap the planet in a dense net of observations in close proximity, approximating measurements on a closed surface about the source (Fig 1), ideal for characterizing potential fields [8].

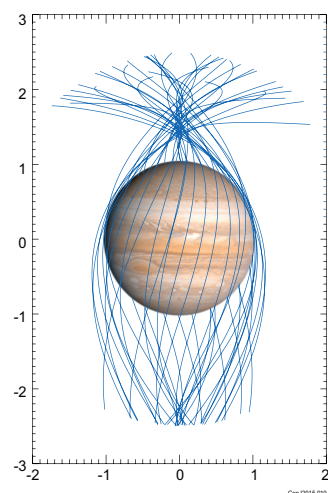


Figure 1: Juno wraps the planet in a dense net of observations, with 32 passes to within $\sim 1.06 R_J$.

Repeated periapsis passes will eventually wrap the planet with observations equally spaced in longitude ($< 12^\circ$ at the equator), optimized for characterization of the Jovian dynamo. Such close passages are sensitive to small spatial scale variations in the magnetic field and a large number of such passes is required to bring the magnetic field into focus. The first few periapsis passes have revealed a magnetic field rich in higher harmonic content, suggestive of magnetic dynamo action not far beneath the surface [7,13]. It is perhaps not surprising that the field observed in close proximity to the planet is very different from that predicted by existing models, necessarily limited to low harmonic degree and order.

Juno was also required to duck beneath Jupiter's hazardous radiation belts, and orbit in a plane close to Jupiter's rotation axis, providing frequent transits of the northern and southern auroral ovals. These and other considerations led to a polar orbit with a period of 53.5 days and apoapsis at $\sim 100 R_J$ radial distance, affording an unprecedented opportunity to explore Jupiter's polar magnetosphere [2]. Thus Juno is also instrumented to characterize particles and fields in the polar magnetosphere [11,12] and to acquire images and spectra of its polar auroras in the infrared [1] and ultraviolet [9]. Juno also carries a visible (and methane band) imager intended primarily for education and public outreach [10].

The magnetic field investigation (MAG) [8] is equipped with two magnetometer sensor suites, located 10 & 12 m from the center of the spacecraft at the end of one of Juno's three solar panel wings. Each contains a vector fluxgate magnetometer (FGM) sensor and a pair of co-located non-magnetic star tracker camera heads, providing accurate attitude determination for the FGM sensors. These cameras monitor the distortion of the mechanical appendage

(solar array and MAG boom) in real time, allowing accurate attitude reconstruction for the FGM sensors to ~20 arcsec throughout the mission [8].

These heavily-shielded camera heads must recognize stars in the presence of penetrating radiation and in so doing also provide a record of penetrating radiation (primarily electrons with energies >10 MeV) with significant science value [3,4]. One of the star cameras also continuously monitors the presence of objects in the field of view that are not among the objects in an on-board star catalog (Non-Stellar-Objects) and stores this information for subsequent retrieval. This capability has allowed us to track ejecta from the spacecraft liberated by the high-velocity (~10 km/s) impacts of interplanetary dust particles (IDPs) detected during cruise from Earth to Jupiter [5]. The same autonomous tracking capability also affords an opportunity to detect and characterize objects in orbit about Jupiter, ranging in size from microns (detected via spacecraft ejecta) to meters (imaged as they transit the FOV).

We present an overview of the magnetic field observations obtained during the first few polar orbits in context with prior observations and those acquired by Juno's other science instruments. We also discuss observations of dust particles encountered both during cruise from Earth to Jupiter and near the Jovian equator. Juno transits the Jovigraphic equator at high speed (60 km/s) and collisions with dust grains vaporize both the grain and part of the Juno spacecraft at the impact site, creating a hot, ionized gas and particulate ejecta. The MAG investigation camera head tracks particle ejecta of sufficient size, if passing through the FOV, while the Waves records the electrical response of the spacecraft, awash in the expanding plasma cloud. The Waves investigation is capable of detecting the numerous impacts of micron-sized dust particles, likely moving inward from Jupiter's ring [14], whereas the camera head detects ejecta liberated by (presumably) less numerous and more massive dust particles.

References

- [1] Adriani, A., Filacchione, G., Di Iorio, T., et al.: JIRAM, the Jovian infrared auroral mapper, *Space Sci. Rev.*, doi 10.1007/s11214-014-0094-y.
- [2] Bagenal, F., Adriani, A., Allegrini, F., et al.: Magnetospheric science objectives of the Juno mission, *Space Sci. Rev.*, doi 10.1007/s11214-014-0036-8.
- [3] Becker, H.N., Alexander, J. A., Adriani, A. et al.: The Juno Radiation Monitoring (RM) Investigation, *Space Sci. Rev.*, doi: 10.1007/s11214-017-0345-9, 2017.
- [4] Becker, H. N., Santos-Costa, D., Jørgensen, J. L., et al.: Observations of high energy electrons in Jupiter's innermost radiation belts and polar regions by the Juno radiation monitoring investigation: Perijoves 1 and 3, *Geophys. Res. Lett.*, doi: 10.1002/2017GL073091, 2017.
- [5] Benn, M., Jørgensen, J. L., Denver, T., et al.: Observations of interplanetary dust by the Juno magnetometer investigation, *Geophys. Res. Lett.*, in press, 2017.
- [6] Bolton, S. J. and the Juno Science Team (2010). The Juno mission. *Proceedings of the International Astronomical Union Symposium*, No. **269**: 92-100.
- [7] Bolton, S. J., Adriani, A., Adumitroaie, V., et al.: Jupiter's interior and deep atmosphere: the first pole-to-pole pass with the Juno spacecraft, *Science*, doi: 10.1126/science.aal2108, 2017.
- [8] Connerney, J. E. P., Benn, M., Bjarno, et al. (2017) The Juno Magnetic Field Investigation, *Space Sci. Rev.*, doi: 10.1007/s11214-017-0334-z.
- [9] Gladstone, G. R., Persyn, S. C., Eterno, J. S., et al.: The ultraviolet spectrograph on NASA's Juno mission, *Space Sci. Rev.*, doi: 10.1007/s11214-014-0040-z.
- [10] Hansen, C. J., Caplinger, M. A., Ingersoll, A., et al.: Junocam: Juno's outreach camera, *Space Sci. Rev.*, doi: 10.1007/s11214-014-0079-x.
- [11] Mauk, B. H., Haggerty, D. K., Jaskulek, S. E., et al.: The Jupiter Energetic Particle Detector Instrument (JEDI) Investigation for the Juno Mission, *Space Sci. Rev.*, doi: 10.1007/s11214-013-0025-3.
- [12] McComas, D. J., Alexander, N., Allegrini, F., et al.: The Jovian auroral distributions experiment (JADE) on the Juno mission to Jupiter, *Space Sci. Rev.*, doi:10.1007/s11214-013-9990-9.
- [13] Moore, K. M., Bloxham, J., Connerney, J. E. P., et al.: The analysis of initial Juno magnetometer data using a sparse magnetic field representation, *Geophys. Res. Lett.*, in press, 2017.
- [14] Connerney, J. E. P., Adriani, A., Allegrini, F., et al., Jupiter's Magnetosphere and Aurorae Observed by the Juno Spacecraft During its First Polar Orbits, *Science*, 10.1126/science.aam5928, 2017.

High altitude ammonia ice clouds observed by Juno/JIRAM at stationary positions

G. Filacchione (1), G. Sindoni (1), A. Adriani (1), A. Mura (1), F. Tosi (1), M. L. Moriconi (2), F. Altieri (1), B.M. Dinelli (2), D. Turrini (1), R. Noshese (1), A. Cicchetti (1), G. Piccioni (1), A. Migliorini (1), F. Fabiano (3), C. Plainaki (4), A. Olivieri (4), S. Bolton (5), S. Atreya (6), J. Lunine (7)

(1) INAF-IAPS, Istituto di Astrofisica e Planetologia Spaziali, Roma, Italy (gianrico.filacchione@iaps.inaf.it), (2) CNR-Istituto di Scienze dell'Atmosfera e del Clima, Bologna e Roma, Italy, (3) Dipartimento di Fisica e Astronomia, Università di Bologna, (4) ASI Agenzia Spaziale Italiana, Roma, Italy, (5) Southwest Research Institute, San Antonio, Texas, USA, (6) University of Michigan, Ann Arbor, Michigan, USA, (7) Cornell University, Ithaca, New York, USA

Abstract

We report the first spectroscopic identification of high altitude ammonia ice clouds observed in three discrete oval structures in the atmosphere of Jupiter by the Jovian InfraRed Auroral Mapper (JIRAM, [1]) on board the Juno spacecraft. The ovals are observed at stationary positions in $2.57 \mu\text{m}$ radiance maps derived from JIRAM's spectrometer channel data acquired on Aug 2th 2016 (observation phase #2) and Aug 25th 2016 (#3) during Juno's first perijove passage. A quantitative analysis of these three features is performed by means of an inversion technique based on Bayesian method.

1. Dataset and data projection

JIRAM spectral channel performs imaging spectroscopy in the $2\text{--}5 \mu\text{m}$ range with 336 bands (spectral sampling $\approx 9 \text{ nm/band}$) and 256 spatial pixels (IFOV= $240 \mu\text{rad}$, FOV= 3.52°). In general consecutive slits are not spatially connected on Jupiter reference surface because the spectrometer can acquire only one frame per each Juno spacecraft rotation (i.e. once every 30 seconds). For this reason it is necessary to project each single frame to build a global map. The method used to build the maps shown in Fig. 1 is the same described in [2]. Each individual JIRAM pixel having incidence and emission angles $\leq 80^\circ$ has been projected on a cylindrical grid map with a resolution of $0.25^\circ/\text{pixel}$ along planetographic longitude and latitude axes. In case of redundancy above a single $0.25^\circ \times 0.25^\circ$ bin, the median value is shown. For brevity we show here only the maps derived from observation phase #3.

2. High altitude ammonia clouds

High altitude ammonia clouds can be identified by means of their elevated radiance at 2.0 and $2.57 \mu\text{m}$ and by simultaneous low radiance at $2.72 \mu\text{m}$ as was done first by Galileo Near Infrared Mapping Spectrometer NIMS [3]. This is indeed the spectral behavior observed also in JIRAM's three ovals that are present in the $2.57 \mu\text{m}$ radiance map shown in Fig. 1-top panel at coordinates (lon = 345° , lat = -33.5°), (lon = 292° , lat = 41.5°) and (lon = 5.5° , lat = 41.5°) for ovals #1, #2, #3, respectively. At the same positions the ovals disappear in the $2.72 \mu\text{m}$ radiance map (Fig. 1-bottom panel). The position of the three ovals is stationary during the 23 days period encompassing JIRAM observation phases #2 (Aug 2th 2016) and #3 (Aug 25th 2016).

3. Spectral Analysis

The average radiance spectra collected in a region of lon - lat of $2^\circ \times 2^\circ$ centered above the position of each oval are shown in 2. These spectra are characterized by high signal at $2 \mu\text{m}$ where clouds reflected sunlight. At the same time their thermal emission in the $4.5\text{--}5 \mu\text{m}$ spectral range is very low, since the clouds have high opacity at these wavelengths. We have performed a quantitative analysis of these spectra by using an inversion technique based on a Bayesian approach. Moreover, we have compared the spectral data collected within the ovals with adjacent ones in order to contextualize the ovals properties relative to their surroundings. The same method has been applied to derive the properties of the White Ovals observed by JIRAM between $-35^\circ \leq \text{lat} \leq -40^\circ$ [4]. The results of the spectral inversion will be discussed at the meeting.

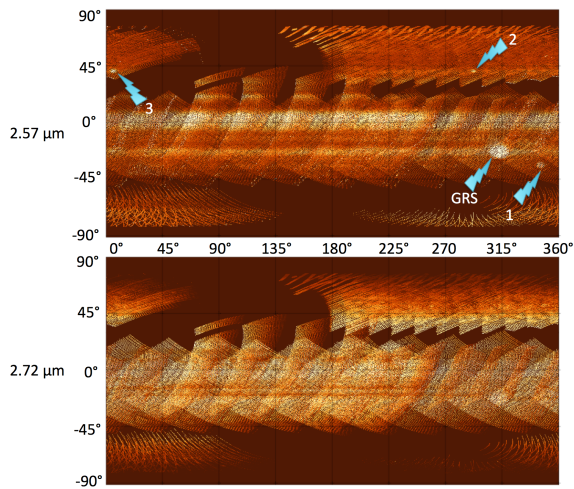


Figure 1: Top panel: Radiance map at $2.57 \mu m$. The positions of the three ovals and Great Red Spot (GRS) are shown. Bottom panel: Radiance map at $2.72 \mu m$.

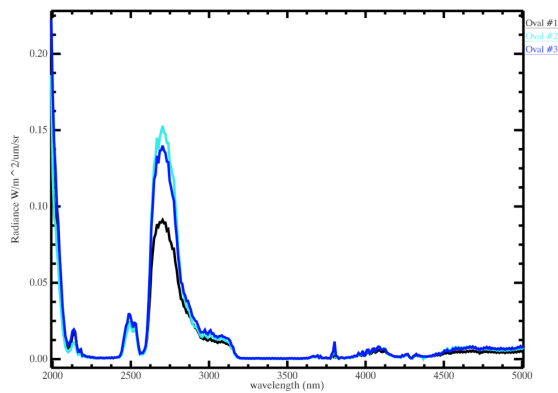


Figure 2: Average spectral radiances of the three ovals calculated within a region of $\text{lon} \times \text{lat}$ of $2^\circ \times 2^\circ$, centered above the position of each oval.

Acknowledgements

The JIRAM project is financially founded by the Italian Space Agency (ASI) with the grant n. 2016-23-H.0 This research has made use of NASA's Astrophysics Data System.

References

- [1] Adriani et al., *Space Sci. Rev.*, doi 10.1007/s11214-014-0094-y, 2004.
- [2] Filacchione, G. et al., *Icarus*, 274, 334-349, 2016.

- [3] Baines, K. H., Carlson, R. W., Kamp, L. M., *Icarus*, 159, 74-94, 2002.
- [4] Sindoni, G. et al. *Geophys. Res. Lett.*, 44, doi:10.1002/2017GL072940, 2017

Junocam Imaging Jupiter: Results from PJ1 through PJ8

M. A. Ravine (1), C. J. Hansen (2), G. S. Orton (3), T. W. Momary (3), M. A. Caplinger (1), S. K. Atreya (4), A.P. Ingersoll (5), S. J. Bolton (6), F. Tabataba-Vakili (3), J. H. Rogers (7) and G. Eichstadt (8).

(1) Malin Space Science Systems, San Diego, California, USA (ravine@msss.com), (2) Planetary Science Institute, Tucson, Arizona, USA, (3) Jet Propulsion Laboratory, California Institute of Technology, Pasadena, California, USA, (4) University of Michigan, Ann Arbor, Michigan, USA, (5) Division of Geological and Planetary Sciences, California Institute of Technology, Pasadena, California, USA, (6) Southwest Research Institute, San Antonio, Texas, USA, (7) British Astronomical Association, London, UK and (8) Independent scholar, Stuttgart, Germany.

Abstract

Juno's imaging system, JunoCam, has acquired images of Jupiter's poles for each of the first eight orbits of the mission, providing a significant quantitative improvement in our coverage of Jupiter's poles and revealing very different atmospheric structure than at the lower latitudes.

1. Introduction

The highly elliptical inclined orbit of the Juno spacecraft, with perijove 5000 km above the cloud tops, provides a geometry for polar imaging much more favorable than previous missions. Juno's imaging system, Junocam, has acquired color images of each of Jupiter's poles for 7 of the first eight perijove passes (PJ1 through PJ8, but not PJ2). These images show an atmospheric circulation very different from the banded structure of the lower latitudes ($<60^\circ$), and the variability of that circulation was sampled at the 53-day period of Juno's orbit.

2. JunoCam Instrument

JunoCam has a single CCD detector with an integral color-strip filter that enables the instrument to image in four color bands—blue, green, red and the 889-nm methane band. The Junocam lens maps a field of view of 58° across the width of the detector, which is perpendicular to the scan direction from spacecraft rotation. Repeated readout of the filtered sections of the CCD with rotation allows Junocam to build up a color image. Junocam's CCD can be operated with Time Delay Integration (TDI) to improve signal levels. Because of the much lower signal levels in the methane band, those images are acquired separately from the RGB images, and with much more TDI. Details are given by Hansen et al. (1)

3. Junocam Polar Imaging

Around each perijove pass of the Juno spacecraft, JunoCam acquires multiple half-disk color images of the North and South Poles at high emission angle ($>70^\circ$). These images have a spatial scale at the cloud tops of ~ 50 km/pixel. The geometry of the orbit accommodates the acquisition of multiple images of the poles over a period of up to one hour enabling the acquisition of brief time-lapse movies of polar features.

The key morphologic feature of Jupiter's polar regions is a breakdown of the east-west banded structure that dominates latitudes less than $\sim 60^\circ$. In the polar regions, the structure is dominated by many discrete, compact features against a background that is darker and more uniform than the structure equatorward of $\sim 60^\circ$ latitude in either hemisphere.

The following discrete features have been observed by JunoCam (and are visible in Figures 1 and 2):

- Circumpolar cyclones: bright, circular, spiral features immediately around the poles. Time-lapse image sequences show they rotate counterclockwise.
- Ovals: bright, oval features with a distribution of diameters down to the Junocam resolution limit (<100 km).
- Folded filaments: bright, amorphous, apparently turbulent features 4,000 to 7,000 km in extent. These appear similar to the much smaller "folded filaments" seen at lower latitudes.

Junocam samples the time development of these features on two different timescales: imaging the

poles multiple times on the same orbit (limited by orbital geometry to < 1 hour) and imaging on successive Juno orbits (separated by 53 days).



Figure 1: Jupiter imaged by Junocam just after the fifth perijove pass (PJ5). The South Pole is about three-quarters of the way to the lower limb. The lower albedo region extends from the pole to $\sim 60^\circ\text{S}$ latitude. Northward of that boundary, the belt-and-zone structure is seen, foreshortened.

4. Summary and Conclusions

JunoCam has acquired observations of Jupiter's poles on eight successive Juno orbits, revealing very different atmospheric features than pertains at lower latitudes. JunoCam will continue these observations for the rest of the Juno Mission. Orton et al. (2) provide a more detailed discussion of the features, as observed in Juno's first perijove.

Acknowledgements

This research was funded by the National Aeronautics and Space Administration through the

Juno Project. A portion of these funds were distributed to the Jet Propulsion Laboratory, California Institute of Technology. All Junocam images can be obtained on the Mission Juno web site (<https://www.missionjuno.swri.edu>). Thanks for the processing of the images in the figures done by Gabriel Fiset (Fig. 1) and Roman Tkachenko (Fig. 2).

References

- [1] Hansen, C. J., et al. Junocam: Juno's outreach camera. *Space Sci. Rev.* 2014. doi10.007/s/11214-014-0079-x
- [2] Orton, G. S., et al. The first close-up images of Jupiter's polar regions: Results from the Juno mission JunoCam instrument. *Geophys. Res. Lett.* 44, 2017. doi: 10.1002/2016GL072443.



Figure 2: Jupiter's North Pole, imaged by Junocam just before Juno's fifth perijove pass (PJ5). As with the South Pole view in Figure 1, the North Pole is surrounded by a lower albedo region with two well-developed folded filaments near the albedo boundary.

Identifying the source of colour and featural changes in Jupiter's atmosphere from MUSE/VLT

A. S. Braude (1), P. G. J. Irwin (1), G. S. Orton (2), L. N. Fletcher (3)

(1) Department of Atmospheric, Oceanic and Planetary Physics, University of Oxford, United Kingdom, (2) Jet Propulsion Laboratory, California Institute of Technology, USA, (3) Department of Physics & Astronomy, University of Leicester, UK

Abstract

MUSE/VLT observations of Jupiter have been made in the visible/near-IR (0.48-0.93 μ m) at high spectral resolution between 2014-2017, providing global context to Juno observations in the mid-IR and microwave, and enabling cloud structure and colour to be better constrained at the level of the visible cloud layers. Significant changes were observed in the appearance of the northern hemisphere of Jupiter in 2017. Changes in cloud structure were modelled using the 'Crème Brûlée' model of Sromovsky et al [5], and using the chromophore of Carlson et al [2] as the main blue-absorber. This model was seen to fit the belt regions of Jupiter well, indicating a predominantly high-altitude source of cloud colour, but a poor fit was seen with respect to the zones due to excessive green-absorption.

1. Introduction

Significant changes in colour and in the general appearance of discrete features on Jupiter have been observed in the past few years, particularly in the northern hemisphere and the Great Red Spot, which is observed to have shrunk in longitudinal size and become redder since 2012 [4]. We attempt to quantify these changes using the MUSE integral-field spectrograph [1], providing comprehensive wavelength coverage in the visible/near-IR (0.48-0.93 μ m), and providing global context to Juno observations in the mid-IR and microwave, in order to further constrain vertical cloud structure at the level of the visible cloud layers, as well as the composition of the 'chromophore' particles that colour Jupiter's belts and Great Red Spot.

2. Modelling and preliminary results

Our data consists of five sets of MUSE spectral image cubes between February 2014 and March 2017. The most noticeable change in Jupiter's appearance is in 2017, when the northern boundary of the North Tropical Zone appears to move southwards, followed by an increase in high-altitude haze, as shown in Figure 1. Our retrievals confirm that the narrowing of the North Tropical Zone is accompanied by a local decrease in tropospheric cloud opacity and an increase in opacity of the chromophore layer, as shown in Figure 2, but this also appears to be accompanied by a reduction in the tropospheric cloud opacity of the Equatorial Zone.

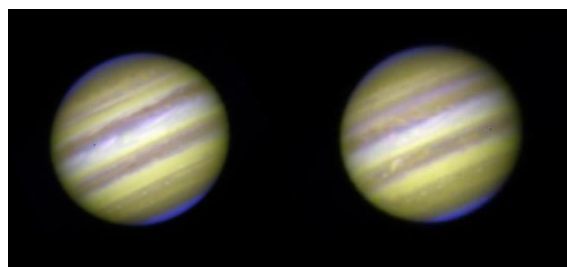


Figure 1: MUSE False colour image of Jupiter in (left) 9th March 2016, (right) 10th January 2017. Regions that are bright at 0.89 μ m are shown in blue

We attempt to replicate the results of Sromovsky et al [5] by modelling a meridional swath of Jupiter's atmosphere using the 'Crème Brûlée' model, consisting of a high-altitude stratospheric haze layer and a thin layer of chromophore with the optical constants of Carlson et al [2] just above an extended tropospheric cloud layer. We find this model generally provides a good fit to the MUSE data in the belt regions, indicating a stratospheric source of colour on Jupiter. However, contrary to the findings of Sromovsky et al, we find that the imaginary

refractive index of the chromophore must be significantly reduced at green wavelengths to provide a good fit in the zones.

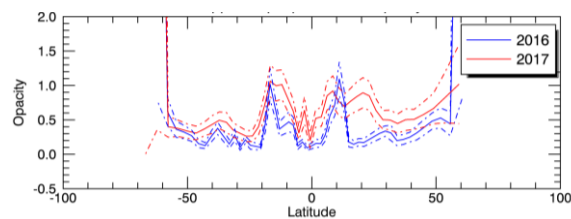


Figure 2: Retrieved change in chromophore opacity along a central meridian of Jupiter between 2016 and 2017

Summary and Conclusions

We use visible/near-IR spectra from MUSE/VLT to constrain cloud structure and colour in Jupiter's troposphere at high spectral resolution, thereby providing global context to localised Juno observations. Significant changes in appearance and cloud structure are observed in the northern hemisphere of Jupiter. We are generally able to provide a good fit to the MUSE spectra using Sromovsky et al's 'Crème Brûlée' model, although we find that the zones of Jupiter are not green-absorbing enough for Carlson et al's chromophore to be a good fit there. Irradiated NH_4SH is unlikely to be the main source of colour in Jupiter's atmosphere, as hypothesised by Loeffler et al [3], due to the absence of $0.6\mu\text{m}$ absorption and a sufficiently large blue-absorption gradient. However, we cannot entirely discount it as a contributor to Jovian colour, perhaps mixed in with the Carlson chromophore layer or in a layer directly below, and we wish to investigate this possibility further in the future once optical constant data become available. We are set to obtain more MUSE observations of Jupiter as the year progresses, and using the aforementioned 'Crème Brûlée' model we wish to further model changes in Jupiter's general appearance, as well as the appearance of the Great Red Spot and other discrete features in Jupiter's atmosphere.

References

- [1] Bacon, R., Accardo, M., Adjali, L., Anwand, H., Bauer, S., Biswas, I., Blaizot, J., Boudon, D., Brau-Nogue, S., Brinchmann, J. and Caillier, P.: The MUSE Second-Generation VLT Instrument, SPIE Astronomical Telescopes + Instrumentation, pp. 773508-773508, 2010.
- [2] Carlson, R. W., Baines, K. H., Anderson, M. S., Filacchione, G., and Simon, A. A.: Chromophores from Photolyzed Ammonia Reacting with Acetylene: Application to Jupiter's Great Red Spot, *Icarus*, Vol. 274, pp. 106-115, 2016.
- [3] Loeffler, M. J., Hudson, R. L., Chanover, N. J., and Simon, A. A.: The spectrum of Jupiter's Great Red Spot: The case for ammonium hydrosulfide (NH_4SH), *Icarus*, Vol. 271, pp. 265-268, 2016.
- [4] Simon, A. A., Wong, M. H., Rogers, J. H., Orton, G. S., De Pater, I., Asay-Davis, X., Carlson, R.W., and Marcus, P. S.: Dramatic Change in Jupiter's Great Red Spot from Spacecraft Observations, *The Astrophysical Journal Letters*, Vol. 797, L31, 2014.
- [5] Sromovsky, L. A., Baines, K. H., Fry, P. M., and Carlson, R. W.: A Possibly Universal Red Chromophore for Modeling Color Variations on Jupiter, *Icarus*, Vol. 291, pp. 232-244, 2017.

Jovian decametric radiation seen from Juno, Cassini, STEREO A, WIND, and Earth-based radio observatories

M. Imai (1), W. S. Kurth (1), G. B. Hospodarsky (1), S. J. Bolton (2), J. E. P. Connerney (3), S. M. Levin (4), A. Lecacheux (5), L. Lamy (5), P. Zarka (5), T. E. Clarke (6), and C. A. Higgins (7)

(1) University of Iowa, Iowa City, Iowa, USA, (2) Southwest Research Institute, San Antonio, Texas, USA, (3) NASA Goddard Space Flight Center, Greenbelt, Maryland, USA, (4) Jet Propulsion Laboratory, California Institute of Technology, Pasadena, California, USA, (5) LESIA, CNRS, Observatoire de Paris, Meudon, France, (6) Naval Research Laboratory, Washington, DC, USA, (7) Middle Tennessee State University, Murfreesboro, Tennessee, USA (masafumi-imai@uiowa.edu / Fax:+1-319-335-1753)

Abstract

Jupiter's decametric (DAM) radiation is generated very close to the local gyrofrequency by the electron cyclotron maser instability (CMI). This type of planetary auroral radiation is common to the other magnetized planets in our solar system (Earth, Saturn, Neptune, and Uranus). Among planetary auroral radio sources, Jupiter's non-thermal DAM radiation represents the strongest with a flux density of 10^{-21} – 10^{-20} W/(m²Hz) at 1 AU over the broadest frequency range from a few to 40 MHz. Depending upon terrestrial ionospheric conditions and radio frequency interference, the DAM emission above 10 MHz is widely detectable from Earth-based radio observatories. In contrast, frequencies observed by spacecraft depend upon receiver capability and the ambient solar wind plasma frequency. Observations of DAM from widely separated observers can be used to investigate the geometrical properties of the beam and learn about the generation mechanism. The first two-point common detections of Jovian DAM radiation were made using the Voyager spacecraft and ground-based radio observatories in early 1979, but, due to geometrical constraints and limited flyby duration, a full understanding of the latitudinal beaming of Jovian DAM radiation remains elusive. Juno first detected Jovian DAM emissions on May 5, 2016, on approach to the Jovian system, initiating a new opportunity to perform observations of common DAM radiation with Juno, Cassini, STEREO A, WIND, and Earth-based radio observatories (Long Wavelength Array Station One (LWA1) in New Mexico, USA, and Nançay Decameter Array (NDA) in France). These observers are widely distributed throughout our solar system and span a broad frequency range of 3.5 to 40.5 MHz. Juno resides in

orbit at Jupiter, Cassini at Saturn, STEREO A in 1 AU orbit, WIND around Earth, and LWA1 and NDA at Earth. Juno's unique polar trajectory is expected to facilitate extraordinary stereoscopic observations of Jovian DAM radiation, leading to a much improved understanding of the latitudinal beaming and the CMI emission mechanism.

Wind field estimation at 5.0 μm by Juno/JIRAM imaging of Jupiter's poles

M. L. Moriconi (2), A. Adriani (1), A. Mura (1), A. Migliorini (1), F. Altieri (1), G. Filacchione (1), B.M. Dinelli (2), F. Tosi (1), F. Fabiano (3), G. Sindoni (1), D. Turrini (1), R. Noschese (1), A. Cicchetti (1), G. Piccioni (1), C. Plainaki (4), A. Olivieri (4), S. Bolton (5), S. Atreya (6), J. Lunine (7)

(1) INAF-Istituto di Astrofisica e Planetologia Spaziali, Roma, Italy (francesca.altieri@iaps.inaf.it), (2) CNR-Istituto di Scienze dell'Atmosfera e del Clima, Bologna e Roma, Italy, (3) Dipartimento di Fisica e Astronomia, Università di Bologna, (4) Agenzia Spaziale Italiana, Roma, Italy, (5) Southwest Research Institute, San Antonio, Texas, USA, (6) University of Michigan, Ann Arbor, Michigan, USA, (7) Cornell University, Ithaca, New York, USA

Abstract

During the JP4 pass on Feb 2nd 2017 the Jovian InfraRed Auroral Mapper (JIRAM, [1]) got many observations of the two Jupiter's poles when the Juno spacecraft at perijove passed at very short distance from the planet. The spatial resolutions of the acquired images ranged from 14 to 90 km/px. The JIRAM imager channel in M band – centered at 4.780 μm with a 480 nm bandwidth – revealed a complex structure of vortices surrounding the two poles. Northern and southern patterns showed a different number of eddies organized in quasi-octagonal and pentagonal geometrical shapes. We apply the optical technique of Particle Image Velocimetry (PIV) to some of the JIRAM images of the two poles to investigate the wind field responsible of those patterns. PIV provides information about the distribution of the two cartesian velocity components of the flow, searching corresponding pixel patterns in two or more successive images and using cross-correlation. We employ the projections of the JIRAM geo-referenced data on a stereo polar plane as measurement plane.

In this work, we present the wind field estimation for two northern and southern Jupiter's polar regions and report in detail the procedure pipeline used to build coherent images for the PIV analysis from the JIRAM imager M acquisitions.

Acknowledgements

The project JIRAM is funded by the Italian Space Agency.

References

- [1] Adriani et al. (2014), JIRAM, the Jovian Infrared Auroral Mapper. Space Sci. Rev., doi 10.1007/s11214-014-0094-y.

Jovian aurora from Juno perijove passes: comparison of ultraviolet and infrared images

J.-C. Gérard (1), B. Bonfond (1), A. Adriani (2), G.R. Gladstone (3), A. Mura (2), D. Grodent (1), M. H. Versteeg (3), T. K. Greathouse (3), V. Hue (3), F. Altieri (2), B.M. Dinelli (4), M.L. Moriconi (4), A. Migliorini (2), A. Radioti (1), S.J. Bolton (3), J.E.P. Connerney (5), S.M. Levin (6), F. Fabiano (7)

(1) Laboratoire de Physique Atmosphérique et Planétaire, STAR Institute, Université de Liège, Belgium, (jc.gerard@ulg.ac.be / Fax: +32 43669729), (2) Istituto di Astrofisica e Planetologia Spaziali, INAF, Roma, Italy, (3) Southwest Research Institute, San Antonio, TX, USA, (4) Istituto di Scienze dell'Atmosfera e del Clima, CNR, Bologna and Roma, Italy, (5) NASA/GSFC, Greenbelt, MD, USA, (6) Jet Propulsion Laboratory, Pasadena, CA, USA, (7) Dipartimento di Fisica e Astronomia, Università di Bologna, Italy; (jc.gerard@ulg.ac.be / Fax: +32-43669729)

1. Introduction

The electromagnetic radiation emitted by the Jovian aurora extends from the X-Rays presumably caused by heavy ion precipitation and electron bremsstrahlung to thermal infrared radiation resulting from enhanced heating by high-energy charged particles. Many observations have been made since the 1990s with the Hubble Space Telescope, which was able to image the H_2 Lyman and Werner bands that are directly excited by collisions of auroral electrons with H_2 . Ground-based telescopes obtained spectra and images of the thermal H_3^+ emission produced by charge transfer between H_2^+ and H^+ ions and neutral H_2 molecules in the lower thermosphere. However, so far the geometry of the observations limited the coverage from Earth orbit and only one case of simultaneous UV and infrared emissions has been described in the literature. The Juno mission provides the unique advantage to observe both Jovian hemispheres simultaneously in the two wavelength regions simultaneously and offers a more global coverage with unprecedented spatial resolution. This was the case.

2. Observations

3. Two remote sensing instruments have collected images of the Jovian aurora during several perijove passes of the Juno spacecraft since August 27, 2016. The UltraViolet Spectrograph (UVS) covers the passband $70 < \lambda < 205$ nm. UVS observes Jupiter for ~10 hours centered on closest approach. The Juno spacecraft spins at a rate of about 1 rotation every 30 seconds and the slit projection describes a series of

swaths, which may be combined to generate global images of the UV aurora by integrating the count rate measured between selected wavelengths. As Juno approaches perijove, the spatial coverage decreases and the spatial resolution increases. A scan mirror with an amplitude of 30° may be used to modify the orientation of the line of sight perpendicular to the Juno spin plane and cover the full region of auroral emission in both hemispheres. Since UVS collects spectra covering both short wavelengths partly absorbed by hydrocarbon and longer wavelengths free of absorption, the combination of images makes it possible to construct map of the UV color ratio. This color ratio is considered as a proxy of the characteristic energy of the accelerated electrons producing the auroral H_2 emission. The Jovian Infrared Auroral Mapper (JIRAM) instrument includes two imager channels. One of them (L band) is centered at $3.455 \mu\text{m}$ and includes some of the bright H_3^+ auroral lines. As for UVS, images are acquired every 30 seconds, but the spatial resolution is significantly higher.

In addition, a spectrometer covering the $2\text{--}5 \mu\text{m}$ region at a mean spectral resolution of 9 nm may be used to simultaneously retrieve the H_3^+ column density and temperature and observed diffuse methane emission. Earlier observations have shown that the H_3^+ ro-vibrational spectrum has several bands in the range $3.0\text{--}5.0 \mu\text{m}$. Best conditions for observation of the H_3^+ ions concentrate in the 3.2 to $4.0 \mu\text{m}$ spectral interval where the intense atmospheric methane absorption band minimizes solar and thermal radiation from the planet are low as

a consequence of, resulting in a maximum auroral contrast against Jupiter's dark disk.

3. Infrared–ultraviolet comparison

Data were collected with both instruments during several perijove passes since August 2016, providing high spatial resolution of auroral structures. It is therefore possible to identify sequences when the two spectral imagers were operated simultaneously and observed the same auroral regions. We shall compare the morphology, brightness and time evolution in the two wavelength domains. Since the resolution of the two sets of images is different, the JIRAM images need to be adapted to the UVS pixel size for detailed comparison.

The H_2 emission is a prompt process resulting from collisions between the downward flux of energetic electrons and the major atmospheric constituent. By contrast, H_3^+ ions are produced by charge transfer from auroral-electron-produced H_2^+ and H^+ ions with neutral H_2 molecules. This IR emission is approximately thermal, so that the intensity of the outgoing radiation depends on both the column density of H_3^+ ions and the temperature distribution in the emitting region. We describe similarities and differences in the morphology and brightness distribution. The time evolution in the two spectral domains will be shown and interpreted in terms of energy of the auroral electrons, time history of the precipitation and lifetime of the H_3^+ ions. They will be complemented with UV color ratio maps that visualize the spatial distribution of the characteristic energy of the primary auroral electrons.

Acknowledgements

This research was funded by the PRODEX programme of the European Space Agency managed in collaboration with the Belgian Federal Science Policy Office (BELSPO). A.R. is supported by the Belgian Fund for Scientific Research (FNRS).